A blood marker for Parkinson's Disease: Neuronal exosome-derived α-synuclein

Annika Kluge (Annika.Kluge@uksh.de)
Department of Neurology, University Hospital Kiel

Josina Bunk
Institute of Biochemistry, Christian-Albrecht-University Kiel

Eva Schaeffer
University Hospital Kiel, Department of Neurology

Alice Drobny
Department of Molecular Neurology, University Hospital Erlangen, Friedrich-Alexander University Erlangen-Nürnberg

Wei Xiang
Friedrich-Alexander-University Erlangen-Nürnberg (FAU)

Henrike Knacke
Department of Neurology, University Hospital Kiel

Simon Bub
Department of Molecular Neurology, University Hospital Erlangen, Friedrich-Alexander University Erlangen-Nürnberg

Wiebke Lückstädt
Institute of Anatomy, Christian-Albrecht-University Kiel https://orcid.org/0000-0002-1698-6770

Philipp Arnold
Institute of Functional and Clinical Anatomy, Friedrich-Alexander-University Erlangen-Nürnberg

Ralph Lucius
Institute of Anatomy, Christian-Albrecht-University Kiel

Daniela Berg
University Hospital Schleswig-Holstein Kiel https://orcid.org/0000-0001-5796-5442

Friederike Zunke
University Hospital Erlangen

Article

Keywords: Parkinson's Disease, biomarker, α-synuclein

Posted Date: August 12th, 2021

DOI: https://doi.org/10.21203/rs.3.rs-783910/v1

A blood marker for Parkinson's Disease: Neuronal exosome-derived α-synuclein

Annika Kluge[1*], Josina Bunk[2], Eva Schaeffer[1], Alice Drobny[3], Wei Xiang[3], Henrike Knacke[1], Simon Bub[3], Wiebke Lückstädt[4], Philipp Arnold[5], Ralph Lucius[4], Daniela Berg[1#], Friederike Zunke[3#*]

[1]Department of Neurology, University Hospital Kiel, Kiel, Germany
[2]Institute of Biochemistry, Christian-Albrecht-University Kiel, Kiel, Germany
[3]Department of Molecular Neurology, University Hospital Erlangen, Friedrich-Alexander University Erlangen-Nürnberg, Erlangen, Germany
[4]Institute of Anatomy, Christian-Albrecht-University Kiel, Kiel, Germany
[5]Institute of Functional and Clinical Anatomy, Friedrich-Alexander-University Erlangen-Nürnberg, Erlangen, Germany
[#]contributed equally

*correspondence: Annika.Kluge@uksh.de; Friederike.Zunke@fau.de

Abstract

To date, no reliable clinically applicable biomarker has been established for Parkinson's disease (PD). Our results indicate that a long hoped blood test for Parkinson's disease may be realized. We here assess the potential of pathological α-synuclein originating from neuron-derived exosomes from blood plasma as a possible biomarker. Following the isolation of neuron-derived exosomes from plasma of PD patients and non-PD individuals immunoblot analyses were performed to detect exosomal α-synuclein. Under native conditions significantly increased signals of disease-associated α-synuclein forms in neuron-derived exosomes were measured in all individuals with PD and clearly distinguished PD samples from controls. By performing a protein misfolding cyclic amplification assay these aggregates could be amplified and seeding could be demonstrated. Moreover, the aggregates exhibited β-sheet-rich structures and showed a fibrillary appearance. Our study demonstrates that the detection of pathological α-synuclein conformers from neuron-derived exosomes from plasma samples has the potential of a promising blood-biomarker of PD.

Keywords: α-synuclein, Parkinson´s disease, biomarker, plasma, extracellular vesicles, neuron-derived exosomes, protein misfolding cyclic amplification.

Introduction

To date the gold-standard to confirm Parkinson's Disease (PD) is the post-mortem detection of misfolded α-synuclein (α-syn) as structural component of Lewy bodies in dopaminergic neurons in the substantia nigra (SN) [1]. However, in the clinical routine the diagnosis of PD is still based on the detection of motor symptoms, supported by imaging techniques and the assessment of concurrent non-motor symptoms and risk factors for PD [2]. Therefore, the correct diagnosis and appropriate therapy is still highly dependent on the professional experience of the examiner, and many epidemiological or post-mortem studies found high

rates of misdiagnoses in PD [3-6]. Another major shortcoming of the clinical approach to diagnose PD is the substantially delayed diagnosis in the course of the disease, as the diagnosis-defining motor symptoms occur only late in the neurodegenerative process, i.e. when more than 50 % of dopaminergic neurons in the SN have already been lost [7]. An earlier detection of the disease, ideally in the prodromal phase before motor symptoms occur, is of utmost importance for the development and application of disease-modifying therapies. Finally, the assessment of clinical symptoms by scales is still used as primary outcome parameter in most clinical trials. This semi-quantitative approach is an imprecise reflection of actual disease progression, depending on a variety of potential confounders such as medication intake, examiner's experience and physical as well as psychological form of the patient on the day of examination.

Taken together, there is an urgent need for an objective and reliable biomarker, to improve the diagnostic accuracy of PD, detect the disease in early stages (preferably in the prodromal state) and monitor disease progression. In this respect, the detection of pathological α-syn as neuropathological hallmark of PD has been in the centre of attention in a wide range of studies [8]. Many studies have focused on the identification of α-syn in accessible peripheral tissues for instance biopsies of the gastrointestinal tract, skin or salivary glands [9-12]. Moreover, there are first promising findings regarding the identification and characterization of pathological α-syn forms in biofluids, such as the cerebrospinal fluid (CSF) [13]. However, apart from still highly varying outcomes regarding sensitivity and specificity, all these techniques are limited due to their invasiveness. Compared to those options an easy and low-risk obtainable medium is blood plasma or serum [14]. With regard to contaminations and inconsistent α-syn levels in the blood [14-18], recent studies focused on extracellular vesicles (EVs) like exosomes (30-100 nm membrane vesicles of endocytic origin) and microvesicles (100 nm-1 µm) [19-21]. EVs released by cells of the central nervous system (CNS) (neuron-derived exosomes, NEs) have the capacity to pass the blood brain barrier (BBB) and transport nucleic acids and proteins including α-syn [20,22]. In this manuscript the terms 'exosomes' and 'extracellular vesicles' will be used interchangeably to denote vesicles, which are released extracellularly and can be isolate from plasma samples. For a more detailed description of exosome nomenclature please see the article of the International Society for Extracellular Vesicles [23].

In this study we combined a specific preparation of NEs and the use of structure-specific antibodies to detect pathological α-syn conformers isolated from the blood of PD patients and compared them to non-PD individuals. Using a protein misfolding cyclic amplification assay (PMCA) [13], we analyzed the detected protein form in its capacity to seed α-syn aggregation and built filamentous structures. In this study we demonstrate for the first time that the detection of pathological α-syn conformers extracted from NEs is possible and can be applied as suitable, easy to assess biomarker for PD that reliably discriminates patients from controls.

Results

Demographics

Plasma samples were collected from 15 patients with PD (mean age 67 years, range 46-84 years) and 15 controls (mean age 75 years, range 50-85 years). There was no age distribution difference among the groups ($p = 0.49$). Mean disease duration of PD patients

was 3 (1-13) years and mean clinical motor symptom score (Movement Disorder Society Unified Parkinson's Disease Rating Scale Part 3, MDS-UPDRS-III) was 26.7. Summarized data of both groups are listed in Table 1; available clinical data for each patient/control is listed in the Extended Data Table 1.

Isolation and detection of EVs from peripheral blood

After gradual centrifugation and exosome precipitation (Fig. 1a), the successful isolation of EVs was confirmed through immunoblotting, dynamic light scattering (DLS) and transmission electron microscopy (TEM). The isolation of EVs was confirmed through dot blot analyses using native plasma samples and comparing them to isolated EVs (PD#1-#2, Ctrl#1-#2) (Fig. 1b, Extended Data Fig. 1a). The exosomal marker CD63 was significantly enriched in samples of EVs after normalization to total protein (Fig. 1c). Increased CD63 levels within the samples of EVs indicated a sufficient protocol for enrichment of EVs. Following the exosomal isolation western blot analyses depicted an increased anti-CD63 antibody signal in both groups (PD#1-#5, Ctrl#1-#5) (Fig. 1d). In comparison with untreated plasma samples, increased signal intensities were detected after isolation of EVs (Extended Data Fig. 1b). Comparing control and PD samples, no significant differences in CD63 levels could be found after normalization to Coomassie Brilliant Blue (CBB) staining (Fig. 1e). Further characterization of the diameter and morphology of EVs was gained by negative stain TEM and showed a homogenous preparation of EVs (Fig. 1f). All images can be found in Extended Data Fig. 1c. Particle size measurement from TEM images showed no differences in EVs between PD and control samples (Extended Data Fig. 1d). Furthermore, DLS measurements confirmed the presence of uniform particles with the size as EVs (Fig. 1g) [19]. Analyzed samples of PD patients and controls showed no differences in mean radius distribution according to the TEM-based size distribution. In summary, we demonstrate the sufficient isolation of EVs from blood plasma samples, exhibiting no differences in size or morphology between PD patients and controls.

Identification of NEs from peripheral blood

The purification of NEs (Fig. 2a) led to a significantly increased signal of L1 cell adhesion molecule (NCAM-L1) when compared to native plasma samples and plasma-derived exosomes (PD#4-#5, Ctrl#4-#5) (Fig. 2b-c; Extended Data Fig. 2b). Unspecific binding to the used beads and/or the anti-NCAM-L1 antibody were excluded using an immunoblot approach (Extended Data Fig. 2a). Comparing NCAM-L1 levels of NEs of PD patients and controls showed no significant differences (Fig. 2c). Next, different isoforms of NCAM-L1 were detected through western blot analyses in samples containing NEs (Ctrl#1-#2, PD#3) (Fig. 2d, Extended Data Fig. 2d). Unspecific binding to the anti-NCAM-L1 antibody and/or the anti-NCAM-L1 antibody with beads were also excluded through western blot analysis (Extended Data Fig. 2c). For both approaches the protocol of NEs-isolation was performed as usual. A significant increase in NCAM-L1 levels was detected for NEs samples (Fig. 2e) and the purification of NEs resulted in a significant increase of other established neuronal markers as synaptophysin [24], the pan-neuronal marker protein gene product 9.5 (PGP9.5, also known as ubiquitin C-terminal hydrolase L1 (UCHL-1)) and neuron-specific enolase (NSE) [25,26], which confirm the homogenous and neuronal origin (Fig. 2f; Extended Data

Fig. 2e, g, h). Additionally, DLS measurements of PD-NEs and Ctrl-NEs showed similar size distributions (Extended Data Fig. 2i). Moreover, the quality of NEs-preparation was also examined by TEM imaging (Extended Data Fig. 2j) indicating uniform characteristics (size and morphology), as shown above for EVs samples (Fig. 1; Extended Data Fig. 2 j, k). Thus, no significant differences between PD patients and controls were measured comparing NCAM-L1 levels by immunoblot analyses. In addition, TEM and DLS studies of NEs revealed no significant differences between both groups.

Detection of α-syn from NEs

α-Syn signals in NEs were visualized through immunoblotting (PD#6-#8, Ctrl#6-#8) (Fig. 3a). Using a C-terminal α-syn antibody (C-20) (detects monomeric α-syn) all tested samples showed similar α-syn signal intensities, without significant differences in signal intensity between PD patients and controls (Fig. 3a, b). The presence of pathological α-syn forms was analyzed through the structure-specific α-syn antibody MJFR-14-6-4-2 (Fig. 3c), that was raised against pathological α-syn oligomers [27]. To preserve structure-specific epitopes, dot blot analyses were performed with samples that were not exposed to reducing or unfolding reagents such as DTT or SDS. The antibody specificity was validated and exhibited concentration-dependent binding to *in vitro* produced α-syn filaments and no interaction with recombinant monomeric α-syn (Extended Data Fig. 3a-c). In addition, unspecific signal and binding of the secondary antibody was excluded (Extended Data Fig. 3d). NEs from PD patients showed significantly increased signal intensity in dot blot analyses utilizing the structure-specific α-syn antibody (MJFR) in comparison to control NEs (PD#5-#6, Ctrl#5-#6) (Fig. 3d, e; Extended Data Fig. 3n). Applying an antibody specific for amyloid protein structures (OC), NEs of PD patients also showed a significant increase in antibody signals compared to control exosomes (PD#5-#6, Ctrl#5-#6) (Fig. 3f, g; Extended Data Fig. 3n). Using the Syn-1 antibody (not confirmation specific), no significant difference in the signal intensity between PD and control samples was detected (PD#5-#6, Ctrl#5-#6) (Fig. 3h, i; Extended Data Fig. 3n). In further dot blot approaches, erythrocyte/hemoglobin levels were analyzed to exclude changes in the red blood cell marker and undesired contamination within the samples. To control for the neuronal origin and uniform quality of the NEs preparation, an established neuronal maker (neuronal nuclear protein, NeuN) was continuously evaluated (Extended Data Fig. 3). Taken together, quantitative analysis of total α-syn in NEs showed no significant differences between PD and controls. However, only the application of pathology-associated antibodies and native sample conditions exhibited increased antibody signals of PD-NEs comparing Ctrl-NEs.

Amplification of pathological plasma exosomal α-syn

Seeding capacity of the detected soluble α-syn species was tested using a PMCA assay optimized for α-syn [28,29]. All data shown in Figure 4 was cured after six rounds of protein amplification. The amyloid protein formation was monitored by an increase in Thioflavin T (ThioT) fluorescence over a time-period of 40 h.
PMCA analyses of native plasma samples of PD and control individuals showed no increase in ThioT signals over time (Fig. 4a) and no differences at the 40 h endpoint measurement (Fig. 4b). In addition, we analyzed the signal intensity after incubation with the MJFR

antibody of the untreated plasma samples before and after PMCA by dot blot analysis (PD#8-#9, Ctrl#8-#9) (Fig. 4c). For both time points no significant signal differences between PD and control plasma samples were detected (Fig. 4c-e). PMCA analysis of plasma-isolated EVs is shown in Figure 4f. After 20 h of incubation, ThioT signals of PD-EVs started to increase significantly in comparison to EVs of control individuals (Fig. 4f). After 30 h ThioT fluorescence signals plateaued until the end of the experiment (40 h). Corresponding dot blot analysis indicated no significant differences in MJFR intensity comparing PD patients and controls before PMCA (PD#5-#6, Ctrl#5-#6) (Fig. h, i). After the sixth round of PMCA, MJFR signals of PD samples were significantly increased in comparison to the control group (Fig. 4h, j). PMCA analyses applying the ThioT signal as read out from NEs derived from PD patients and controls are shown in Figure 4k (PD#3-#4, Ctrl#3-#4). After 20 h of incubation ThioT signals started to increase significantly in samples with NEs from PD patients in comparison to samples from control individuals (Fig. 4k). After 30 h ThioT fluorescence plateaued and was stable until the end of the experiment at 40 h. Dot blot analyses, applying the structure specific MJFR antibody, showed signal intensities for NEs derived from PD patient samples that had no overlap with samples from control patients and were significantly different by statistical analysis (Fig. 4m, n). The same could be validated after PMCA, and both groups could be clearly separated by their α-syn signal utilizing the MJFR antibody (Fig. 4m, o). Individual ThioT signal curves of all analyzed samples (native plasma, EVs, NEs) of PD patients (red, n=15) and controls (grey, n=15) subjected to the sixth PMCA round are depicted in Extended Data Fig. 3g-i.

Amplified pathological α-syn forms derived from EVs were further characterized by circular dichroism (CD) spectroscopy. CD spectroscopy of the α-syn conformers derived after the sixth round of PMCA showed a minimum extension around 220 nm indicating the presence of predominantly β-sheet rich structures in samples derived from PD patients (Fig. 4p). In contrast, spectra of analyzed control samples did not exhibit β-sheet characteristics and rather suggest unfolded protein, which would be expected for α-syn monomers (Fig. 4p). Spectra of all analyzed PD patients (PD#1-#3) and controls (Ctrl#1-#3) are shown in Extended Data Fig. 3p. Next, aggregated α-syn after PMCA was visualized through silver staining after denaturing SDS-PAGE (Extended Data Fig. 3q). For this purpose, PMCA end products were centrifuged (sedimented) and resulting pellets were re-suspended, subjected to electrophoresis before silver staining followed. For all analyzed PD samples (PD#4-#7), this resulted in a protein band at ~16 kDa (black arrow), corresponding to the size of monomeric α-syn (Extended Data Fig. 3q). Silver staining of PMCA-α-syn derived from EVs is shown in the lower part of Extended Data Fig. 3q. To visualize formed α-syn structures, TEM imaging was applied on amplified α-syn conformers after six rounds of PMCA and fibrillary structures/aggregates were observed in NEs derived from PD plasma (PD#1) (Fig. 4r). No α-syn multimers could be found after PMCA of Ctrl-NEs (Extended Data Fig. 3r (Ctrl#1)). Altogether, our data demonstrates the ability of soluble α-syn conformers derived from PD-NEs to seed amyloid protein aggregation. Biochemical, biophysical as well as morphological analyses reveal that this NEs-derived α-syn species exhibits β-sheet rich conformations and is organized into fibrils.

Discussion

The results of our study clearly demonstrate that a pathological α-syn form can be extracted and amplified from NEs derived from blood plasma of PD patients. The biochemical and biophysical characterization of the detected α-syn conformers defined β-sheet and amyloid

rich characteristics of NEs-α-syn. This pathological α-syn conformer was detected in all PD patients analyzed without any exception and clearly distinguished PD samples from the control group and vice versa. Moreover, we show the *in vitro* seeding capacity of the NEs-associated CNS-derived α-syn forms, which is known to be specific for pathological α-syn conformation [28,29]. We conclude that the detection and amplification of pathological α-syn conformers in plasma-NEs is a highly promising candidate for a reliable pre-mortem biomarker for PD.

Regarding the urgent need for a biomarker of PD, the detection of α-syn in biofluids has been at the centre of attention in the last years. Several reports demonstrated mostly consistent findings regarding the detection of α-syn in CSF (lower α-syn concentrations in patients with PD), but the invasive nature of lumbar punctures limit the clinical practicability in the routine [30-32]. Moreover, further limitations like large variations in CSF total α-syn values between studies and falsely increased values by blood contaminations must be considered [32,33]. Hence, several meta-analyses show limited sensitivity and specificity [34,35]. Studies analyzing α-syn levels in blood serum or plasma showed inconsistent findings and the risk of erythrocyte contamination or measurement of intra-erythrocyte α-syn species [15,17,20,32,36].

Importantly, recent literature provides evidence that CNS-derived α-syn is able to enter the blood stream within EVs [20,22]. EVs can be classified by their origin and size as smaller exosomes (30-100 nm) and larger microvesicles (100-1,000 nm) [37-39]. The origin of the exosome-subspecies is defined within the endosomal network [39]. Briefly, they are formed by inward budding of limiting membranes or multi-vesicular bodies (MVBs), which release exosomes by fusing with the plasma membrane [39]. First, by inward budding of the cell membrane early endosomes are formed. These endosomes mature into late endosomes or MVBs, in which EVs originate as intraluminal vesicles [40]. After fusing with the cell membrane intraluminal vesicles are released into the extracellular milieu and are called EVs [40]. EVs are released by most cell types and may carry unique, disease-specific cargo [20,39,41,42]. One of the key characteristics of EVs is their ability to pass the BBB and travel between CNS and peripheral circulation [43,44]. Some of their functions such as cell-to-cell communication and contribution to synaptic plasticity or maintenance of myelination have been described before [19,38,45]. Recent studies could detect EVs and NEs in blood and other body fluids *in vivo* and demonstrate their potential as source of biomarkers for neurodegenerative diseases [19,20,45-47].

One of the major advances we demonstrate here is the establishment of an effective method to isolate neuronal EVs (NEs) from plasma without time-consuming (ultra-) centrifugation steps. So far, the most common method to isolate EVs still contain plasma proteins and protein aggregates, which has been discussed as limiting factors for the diagnostic evaluation [39,48,49]. In order to obtain NEs we used an immune-affinity capturing protocol to isolate exosomes, containing NCAM-L1, from all plasma-derived EVs. NCAM-L1 is one of the cell adhesion molecules expressed primarily in the CNS. Moreover, NCAM-L1 is also a specific surface marker of NEs [46,50,51]. Determining the concentration of plasma-derived EVs and the portion of corresponding NEs, we were able to calculate a fraction of 2-6 % NEs of all EVs to belong to the NEs-pool of vesicles with no significant differences in NEs concentrations between PD samples and controls. For both groups, EVs and its subgroup NEs, we were able to verify their isolation by TEM and show by DLS measurements the presence of particles in the size of EVs. There was no significant difference in the diameters of vesicles between EVs and NEs in PD versus controls. These results indicate, that the pathophysiological processes in PD do not alter the approximate number or the size of NEs.

To get further insights in PD associated changes in NEs-cargo, we evaluated α-syn levels within the NEs from PD patients and controls. For both groups we could detect similar total α-syn levels by immunoblotting (Syn-1). Several studies demonstrated no robust α-syn distribution in plasma samples of PD patients and control subjects [36,52]. Interestingly, some studies detected a higher level of α-syn in NEs in PD patients by ELISA and Luminex assays or mass spectrometry and multiplexed electrochemiluminescence compared to healthy controls, which was not seen in our experiments using common standard methods like immunoblotting [20,47,53]. As major limitations in previous studies, contamination of abundant α-syn of peripheral cells like blood cells was described [20,36,47,54].

Compared to these technically rather sophisticated and expensive methods, we here established a clinically more practicable protocol to differentiate between pathological and physiological α-syn conformers. For this, we performed fractional separation of NEs lysate separating soluble from insoluble proteins. Soluble supernatants were further analysed by immunoblotting under native conditions (non-denatured) using a conformation-specific α-syn antibody (MJFR-14-6-4-2), that has been described to bind with high affinity to filamentous and oligomeric α-syn species [27,55]. Applying this protocol, we could demonstrate the presence of an α-syn form that is positive for the conformation-specific antibody (MJFR-14-6-4-2) in all PD-NEs samples. The MJFR signal intensity was approximately 11-fold increased in PD samples compared to Ctrl-NEs, allowing a clear differentiation between PD and control groups. This difference offers the potential to define clear intervals of intensity for PD patient and control groups that could be transferred into a reliable diagnostic tool. Taken together, our findings are based on a strict sequence and essential combination of experimental steps containing the isolation of NEs and subsequent analysis of the soluble fraction under native conditions with an antibody that detects pathological α-syn species. Importantly, no differences using an antibody detecting total α-syn levels (Syn-1 antibody) could be observed, when performing western blot analysis.

In addition to the detection of a pathological α-syn form, we amplified CNS-derived α-syn species from NEs by adjusting a PMCA protocol [28,29]. Hence, our findings demonstrate the seeding capacity of exosomal α-syn species. We thus could illustrate the superior seeding capacity of NEs compared to untreated plasma or EVs to analyze α-syn pathology. This is further underlined by comparing MJFR antibody signal intensities. Untreated plasma samples did not show any significant differences between controls and PD patients before and after PMCA. However, we could show incipient differences in MJFR antibody signal intensities between controls and PD patients for EVs after six rounds of PMCA and a substantial increase of the difference after analyzing NEs. NEs showed the strongest MJFR signals as well as the strongest seeding capacity, presumably constituted by their direct origin in the CNS, indicating that NEs may be considered an ideal matrix for the investigation of brain-associated pathologies [37,47,56,57].

Structural characterization of the PMCA-derived conformers by TEM analyses, CD measurements and immunoblotting revealed β-sheet rich conformations and a fibril-like organization of α-syn that further aggregates into thick fibrillary structures of higher orders. Compared to other α-syn species described in PD patients, our findings demonstrate a similar structural constitution as pathological α-syn derived from CSF or the brain of PD patients [13,58]. Earlier studies demonstrated that different aggregate structures of α-syn cause different effects and different diseases [13,59]. The various α-syn conformers show different

seeding capacities and toxic effects on surrounding cell-types [60]. Therefore, the structural characterization of aggregates is important.

We consider this study as a proof of concept to differentiate plasma of PD patients from that of controls by the protocol described to isolate NEs and amplify pathological α-syn species by PMCA. Future studies will need to validate this protocol in larger cohorts. Moreover, comparison of findings derived from plasma-NEs to α-syn species from brain tissue and CSF will be needed. We are also aware that this study is only the beginning of demonstrating NEs-derived pathological α-syn species as biomarker for PD. Further studies will be necessary to validate our findings in different stages of PD to evaluate whether NEs-derived α-syn may serve as progression marker and to see, whether it is already detectable in the very early - prodromal - stages. Also, plasma samples of other α-synucleinopathies including samples of patients with dementia with Lewy bodies and multiple system atrophy will need to be investigated to elaborate possible similarities or differences between these disease entities.

Conclusion

In summary, we demonstrate for the first time that pathological α-syn detected in plasma-derived NEs can serve as a biomarker to differentiate PD patients from healthy controls. Further confirmation of the presence of pathological α-syn was reached by amplification and visualizing of the aggregates. Our study supports the approach that instead of focusing on quantitative α-syn level in body fluids or tissues, the detection of pathological neural α-syn conformers should be targeted.

References

1. Braak, H., *et al.* Staging of brain pathology related to sporadic Parkinson's disease. *Neurobiol Aging* **24**, 197-211 (2003).
2. Postuma, R.B., *et al.* Validation of the MDS clinical diagnostic criteria for Parkinson's disease. *Movement disorders : official journal of the Movement Disorder Society* **33**, 1601-1608 (2018).
3. Hughes, A.J., Daniel, S.E., Kilford, L. & Lees, A.J. Accuracy of clinical diagnosis of idiopathic Parkinson's disease: a clinico-pathological study of 100 cases. *Journal of neurology, neurosurgery, and psychiatry* **55**, 181-184 (1992).
4. Jain, S., Lo, S.E. & Louis, E.D. Common misdiagnosis of a common neurological disorder: how are we misdiagnosing essential tremor? *Archives of neurology* **63**, 1100-1104 (2006).
5. Newman, E.J., *et al.* Accuracy of Parkinson's disease diagnosis in 610 general practice patients in the West of Scotland. *Movement disorders : official journal of the Movement Disorder Society* **24**, 2379-2385 (2009).
6. Schrag, A., Ben-Shlomo, Y. & Quinn, N. How valid is the clinical diagnosis of Parkinson's disease in the community? *Journal of neurology, neurosurgery, and psychiatry* **73**, 529-534 (2002).
7. Riederer, P., *et al.* alpha-Synuclein in Parkinson's disease: causal or bystander? *J Neural Transm (Vienna)* **126**, 815-840 (2019).
8. Atik, A., Stewart, T. & Zhang, J. Alpha-Synuclein as a Biomarker for Parkinson's Disease. *Brain pathology (Zurich, Switzerland)* **26**, 410-418 (2016).
9. Beach, T.G., *et al.* Multicenter Assessment of Immunohistochemical Methods for Pathological Alpha-Synuclein in Sigmoid Colon of Autopsied Parkinson's Disease and Control Subjects. *J Parkinsons Dis* **6**, 761-770 (2016).
10. Bloch, A., Probst, A., Bissig, H., Adams, H. & Tolnay, M. Alpha-synuclein pathology of the spinal and peripheral autonomic nervous system in neurologically unimpaired elderly subjects. *Neuropathol Appl Neurobiol* **32**, 284-295 (2006).
11. Manne, S., *et al.* Blinded RT-QuIC Analysis of α-Synuclein Biomarker in Skin Tissue from Parkinson's Disease Patients. *Movement disorders : official journal of the Movement Disorder Society* **35**, 2230-2239 (2020).
12. Beach, T.G., *et al.* Multi-organ distribution of phosphorylated alpha-synuclein histopathology in subjects with Lewy body disorders. *Acta neuropathologica* **119**, 689-702 (2010).
13. Shahnawaz, M., *et al.* Discriminating alpha-synuclein strains in Parkinson's disease and multiple system atrophy. *Nature* **578**, 273-277 (2020).
14. Mehta, S.H. & Adler, C.H. Advances in Biomarker Research in Parkinson's Disease. *Current neurology and neuroscience reports* **16**, 7 (2016).
15. Lee, P.H., *et al.* The plasma alpha-synuclein levels in patients with Parkinson's disease and multiple system atrophy. *Journal of neural transmission (Vienna, Austria : 1996)* **113**, 1435-1439 (2006).
16. Foulds, P.G., *et al.* Phosphorylated α-synuclein can be detected in blood plasma and is potentially a useful biomarker for Parkinson's disease. *FASEB journal : official publication of the Federation of American Societies for Experimental Biology* **25**, 4127-4137 (2011).
17. Li, Q.X., *et al.* Plasma alpha-synuclein is decreased in subjects with Parkinson's disease. *Experimental neurology* **204**, 583-588 (2007).
18. El-Agnaf, O.M., *et al.* Detection of oligomeric forms of alpha-synuclein protein in human plasma as a potential biomarker for Parkinson's disease. *FASEB journal : official publication of the Federation of American Societies for Experimental Biology* **20**, 419-425 (2006).
19. Budnik, V., Ruiz-Cañada, C. & Wendler, F. Extracellular vesicles round off communication in the nervous system. *Nature reviews. Neuroscience* **17**, 160-172 (2016).
20. Shi, M., *et al.* Plasma exosomal α-synuclein is likely CNS-derived and increased in Parkinson's disease. *Acta neuropathologica* **128**, 639-650 (2014).

21. Niu, M.*, et al.* A longitudinal study on α-synuclein in plasma neuronal exosomes as a biomarker for Parkinson's disease development and progression. *European journal of neurology* **27**, 967-974 (2020).
22. Shi, M., Sheng, L., Stewart, T., Zabetian, C.P. & Zhang, J. New windows into the brain: Central nervous system-derived extracellular vesicles in blood. *Progress in neurobiology* **175**, 96-106 (2019).
23. Théry, C.*, et al.* Minimal information for studies of extracellular vesicles 2018 (MISEV2018): a position statement of the International Society for Extracellular Vesicles and update of the MISEV2014 guidelines. *Journal of extracellular vesicles* **7**, 1535750 (2018).
24. Sun, B., Dalvi, P., Abadjian, L., Tang, N. & Pulliam, L. Blood neuron-derived exosomes as biomarkers of cognitive impairment in HIV. *Aids* **31**, F9-f17 (2017).
25. Nekludov, M., Bellander, B.M., Gryth, D., Wallen, H. & Mobarrez, F. Brain-Derived Microparticles in Patients with Severe Isolated TBI. *Brain injury* **31**, 1856-1862 (2017).
26. Goetzl, E.J.*, et al.* Altered levels of plasma neuron-derived exosomes and their cargo proteins characterize acute and chronic mild traumatic brain injury. *Faseb j* **33**, 5082-5088 (2019).
27. Kumar, S.T.*, et al.* How specific are the conformation-specific alpha-synuclein antibodies? Characterization and validation of 16 alpha-synuclein conformation-specific antibodies using well-characterized preparations of alpha-synuclein monomers, fibrils and oligomers with distinct structures and morphology. *Neurobiol Dis* **146**, 105086 (2020).
28. Paciotti, S., Bellomo, G., Gatticchi, L. & Parnetti, L. Are We Ready for Detecting α-Synuclein Prone to Aggregation in Patients? The Case of "Protein-Misfolding Cyclic Amplification" and "Real-Time Quaking-Induced Conversion" as Diagnostic Tools. *Frontiers in neurology* **9**, 415 (2018).
29. Shahnawaz, M.*, et al.* Development of a Biochemical Diagnosis of Parkinson Disease by Detection of α-Synuclein Misfolded Aggregates in Cerebrospinal Fluid. *JAMA neurology* **74**, 163-172 (2017).
30. Mollenhauer, B.*, et al.* Direct quantification of CSF alpha-synuclein by ELISA and first cross-sectional study in patients with neurodegeneration. *Exp Neurol* **213**, 315-325 (2008).
31. Tokuda, T.*, et al.* Decreased alpha-synuclein in cerebrospinal fluid of aged individuals and subjects with Parkinson's disease. *Biochem Biophys Res Commun* **349**, 162-166 (2006).
32. Hong, Z.*, et al.* DJ-1 and alpha-synuclein in human cerebrospinal fluid as biomarkers of Parkinson's disease. *Brain* **133**, 713-726 (2010).
33. Mollenhauer, B.*, et al.* Biological confounders for the values of cerebrospinal fluid proteins in Parkinson's disease and related disorders. *Journal of neurochemistry* **139 Suppl 1**, 290-317 (2016).
34. Eusebi, P.*, et al.* Diagnostic utility of cerebrospinal fluid α-synuclein in Parkinson's disease: A systematic review and meta-analysis. *Movement disorders : official journal of the Movement Disorder Society* **32**, 1389-1400 (2017).
35. Gao, L.*, et al.* Cerebrospinal fluid alpha-synuclein as a biomarker for Parkinson's disease diagnosis: a systematic review and meta-analysis. *The International journal of neuroscience* **125**, 645-654 (2015).
36. Shi, M.*, et al.* Significance and confounders of peripheral DJ-1 and alpha-synuclein in Parkinson's disease. *Neuroscience letters* **480**, 78-82 (2010).
37. Coleman, B.M. & Hill, A.F. Extracellular vesicles--Their role in the packaging and spread of misfolded proteins associated with neurodegenerative diseases. *Seminars in cell & developmental biology* **40**, 89-96 (2015).
38. Yáñez-Mó, M.*, et al.* Biological properties of extracellular vesicles and their physiological functions. *Journal of extracellular vesicles* **4**, 27066 (2015).
39. Xu, R., Greening, D.W., Zhu, H.J., Takahashi, N. & Simpson, R.J. Extracellular vesicle isolation and characterization: toward clinical application. *The Journal of clinical investigation* **126**, 1152-1162 (2016).

40. Klingeborn, M., Dismuke, W.M., Bowes Rickman, C. & Stamer, W.D. Roles of exosomes in the normal and diseased eye. *Progress in retinal and eye research* **59**, 158-177 (2017).
41. Simpson, R.J., Lim, J.W., Moritz, R.L. & Mathivanan, S. Exosomes: proteomic insights and diagnostic potential. *Expert review of proteomics* **6**, 267-283 (2009).
42. Fujita, Y., Yoshioka, Y. & Ochiya, T. Extracellular vesicle transfer of cancer pathogenic components. *Cancer science* **107**, 385-390 (2016).
43. Alvarez-Erviti, L*., et al.* Delivery of siRNA to the mouse brain by systemic injection of targeted exosomes. *Nature biotechnology* **29**, 341-345 (2011).
44. Matsumoto, J*., et al.* Transmission of α-synuclein-containing erythrocyte-derived extracellular vesicles across the blood-brain barrier via adsorptive mediated transcytosis: another mechanism for initiation and progression of Parkinson's disease? *Acta neuropathologica communications* **5**, 71 (2017).
45. Lee, T.H*., et al.* Microvesicles as mediators of intercellular communication in cancer--the emerging science of cellular 'debris'. *Seminars in immunopathology* **33**, 455-467 (2011).
46. Simpson, R.J., Kalra, H. & Mathivanan, S. ExoCarta as a resource for exosomal research. *Journal of extracellular vesicles* **1**(2012).
47. Zhao, Z.H*., et al.* Increased DJ-1 and α-Synuclein in Plasma Neural-Derived Exosomes as Potential Markers for Parkinson's Disease. *Frontiers in aging neuroscience* **10**, 438 (2018).
48. Mateescu, B*., et al.* Obstacles and opportunities in the functional analysis of extracellular vesicle RNA - an ISEV position paper. *Journal of extracellular vesicles* **6**, 1286095 (2017).
49. Sódar, B.W*., et al.* Low-density lipoprotein mimics blood plasma-derived exosomes and microvesicles during isolation and detection. *Scientific reports* **6**, 24316 (2016).
50. Fauré, J*., et al.* Exosomes are released by cultured cortical neurones. *Molecular and cellular neurosciences* **31**, 642-648 (2006).
51. Kenwrick, S., Watkins, A. & De Angelis, E. Neural cell recognition molecule L1: relating biological complexity to human disease mutations. *Human molecular genetics* **9**, 879-886 (2000).
52. Foulds, P.G*., et al.* A longitudinal study on α-synuclein in blood plasma as a biomarker for Parkinson's disease. *Scientific reports* **3**, 2540 (2013).
53. Jiang, C*., et al.* Serum neuronal exosomes predict and differentiate Parkinson's disease from atypical parkinsonism. *Journal of neurology, neurosurgery, and psychiatry* **91**, 720-729 (2020).
54. Barbour, R*., et al.* Red blood cells are the major source of alpha-synuclein in blood. *Neuro-degenerative diseases* **5**, 55-59 (2008).
55. Lassen, L.B*., et al.* ELISA method to detect alpha-synuclein oligomers in cell and animal models. *PLoS One* **13**, e0196056 (2018).
56. Thompson, A.G*., et al.* Extracellular vesicles in neurodegenerative disease - pathogenesis to biomarkers. *Nature reviews. Neurology* **12**, 346-357 (2016).
57. Yuyama, K., Sun, H., Mitsutake, S. & Igarashi, Y. Sphingolipid-modulated exosome secretion promotes clearance of amyloid-β by microglia. *The Journal of biological chemistry* **287**, 10977-10989 (2012).
58. Van der Perren, A*., et al.* The structural differences between patient-derived alpha-synuclein strains dictate characteristics of Parkinson's disease, multiple system atrophy and dementia with Lewy bodies. *Acta Neuropathol* **139**, 977-1000 (2020).
59. Peng, C*., et al.* Cellular milieu imparts distinct pathological α-synuclein strains in α-synucleinopathies. *Nature* **557**, 558-563 (2018).
60. Bousset, L*., et al.* Structural and functional characterization of two alpha-synuclein strains. *Nature communications* **4**, 2575 (2013).
61. Zunke, F*., et al.* Reversible Conformational Conversion of alpha-Synuclein into Toxic Assemblies by Glucosylceramide. *Neuron* **97**, 92-107 e110 (2018).
62. Xiang, W*., et al.* Posttranslational modification and mutation of histidine 50 trigger alpha synuclein aggregation and toxicity. *Molecular neurodegeneration* **10**, 8 (2015).

63. Paleologou, K.E*., et al.* Phosphorylation at Ser-129 but not the phosphomimics S129E/D inhibits the fibrillation of alpha-synuclein. *The Journal of biological chemistry* **283**, 16895-16905 (2008).
64. Arnold, P*., et al.* Antigenic and 3D structural characterization of soluble X4 and hybrid X4-R5 HIV-1 Env trimers. *Retrovirology* **11**, 42 (2014).
65. Lückstädt, W*., et al.* Cell Surface Processing of CD109 by Meprin β Leads to the Release of Soluble Fragments and Reduced Expression on Extracellular Vesicles. *Frontiers in cell and developmental biology* **9**, 622390 (2021).

Figures and Tables

Table 1: Clinical parameters of analyzed cohorts

Shown are mean values with indication of SD, mean values with indication of range and *n* (%). Statistics were determined by unpaired two-tailed Student´s t-test and Fisher´s exact test. n.s., not significant; n.a., not applicable.

Category	**PD** (n=15)	**Ctrl** (n=15)	**p-value**
Age (years)	67 (46-84)	75 (50-85)	p=0.49
Male gender, *n* (%)	11 (73 %)	8 (53 %)	p=0.45
Disease duration (years)	3 (1-13)	n.a.	n.a.
Hoen & Yahr (pts)	2.1 (1.1)	n.a.	n.a.
MDS-UPDRS-III (pts)	26.7 (17.3)	n.a.	n.a.

Figure 1

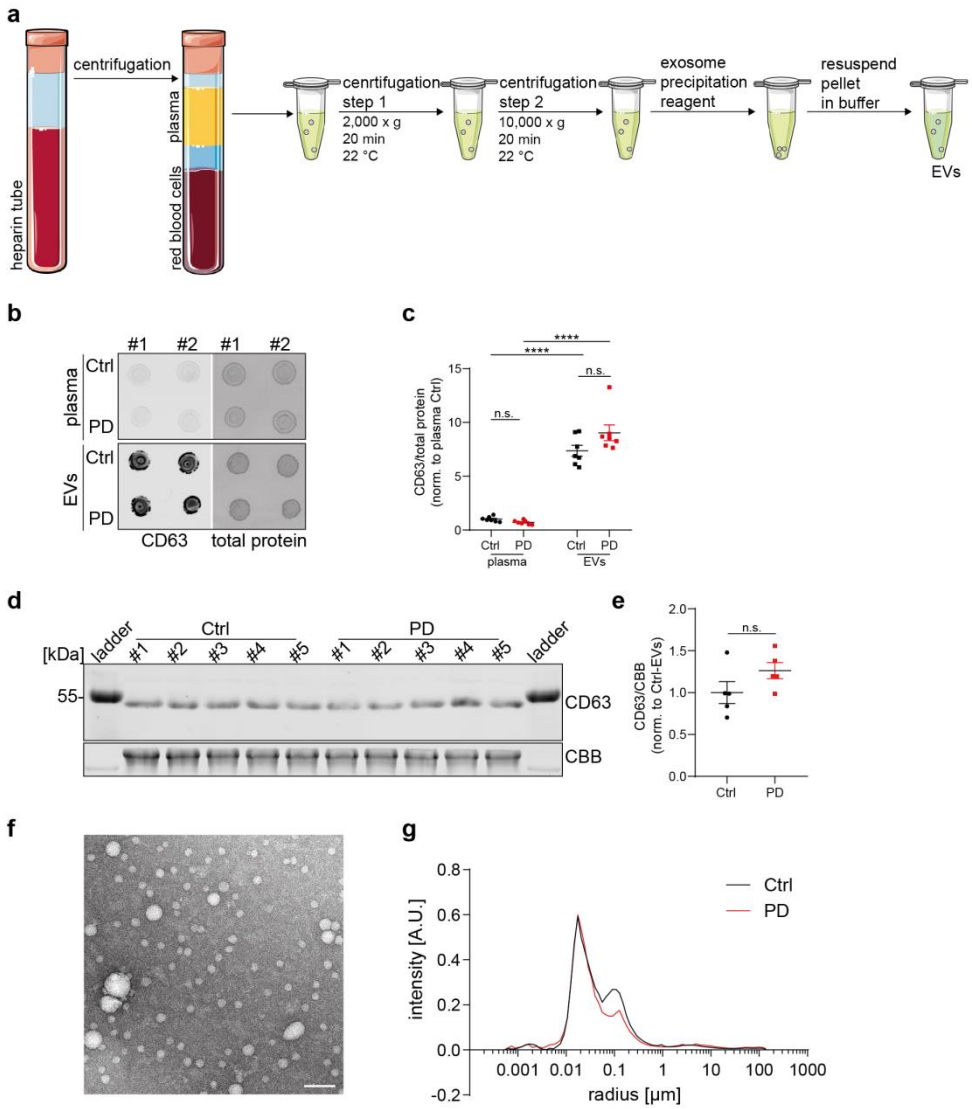

Figure 1: Isolation and characterization of plasma-derived extracellular vesicles (EVs).

a, Schematic illustration of used protocol to isolate EVs from human plasma samples. Blood of Parkinson´s disease (PD) patients and controls was collected. After several centrifugation steps and treatment with the exosome precipitation reagent EVs were purified. **b**, Representative dot blot analyses of plasma samples and plasma-derived EVs. Further dot blots are shown in Extended Data Fig. 1a. Samples were dot-blotted under native conditions and stained with anti-CD63 antibody. As loading control total protein was used. **c**, Quantification of CD63 signal intensity normalized to total protein. Each data point represents one individual PD patient (red) or control individual (black) (*n*=7). **d**, Representative immunoblot of EVs from PD patients and controls. Samples were stained for CD63 (~50 kDa). Coomassie Brilliant Blue staining (CBB) was used as loading control. **e**, Quantification of CD63 signal intensity normalized to CBB. Each data point represents individual patient (red) or control (black) (*n*=5). **f**, Representative transmission electron micrograph from EVs of a control individual. Scale bar = 100 nm. Images of analyzed samples and related size distribution measurements can be found in Extended Data Fig. 1c, d. **g**, Representative dynamic light scattering (DLS) measurement of particle size

distribution of plasma-EVs from PD patients (red) and controls (black) (*n*=3). Statistical analyses were performed using unpaired two-tailed Student's t-test and/or one-way ANOVA with Tukey multiple comparison test. Data are shown as mean ± s.e.m. and statistical significance was specified in terms of n.s. not significant and ****p<0.0001.

Figure 2

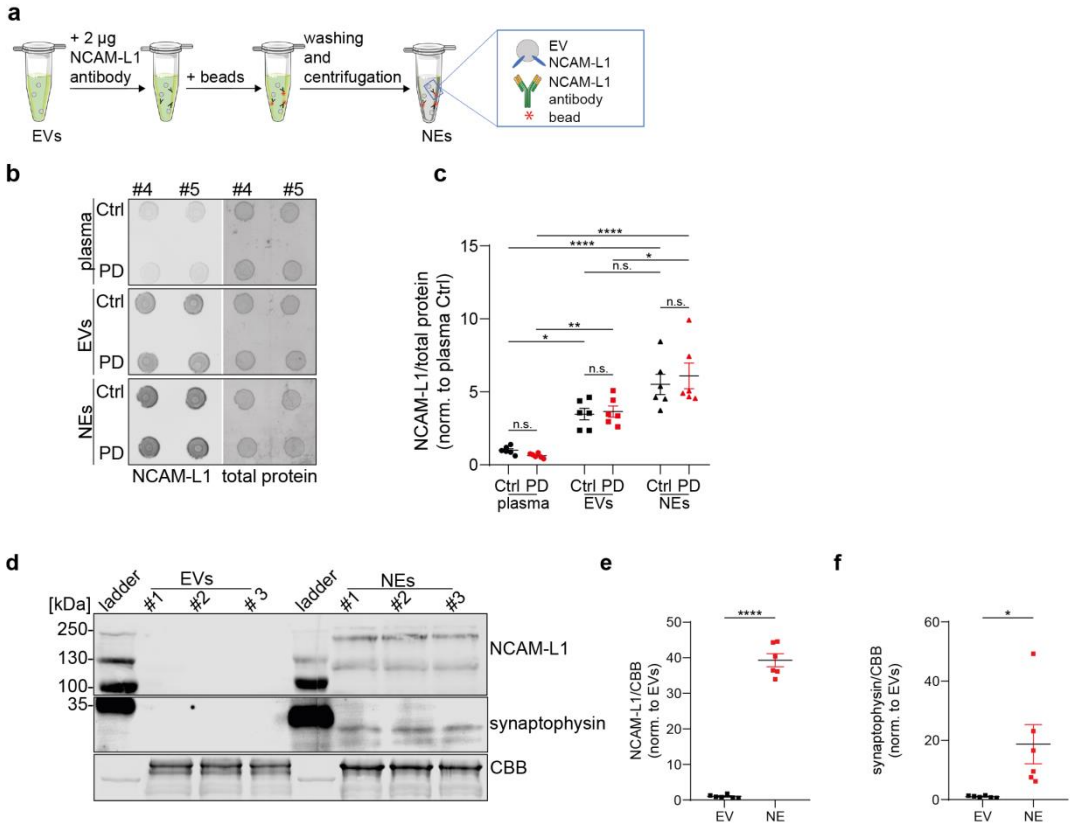

Figure 2: Isolation of neuron-derived exosomes (NEs) and comparison to EVs.

a, Schematic figure of the isolation of NEs using an immune-affinity capturing protocol. Vesicles containing the L1 cell adhesion molecule (NCAM-L1) were precipitated. **b**, Representative dot blot of untreated plasma samples, EVs and NEs showing the enrichment of the used neuronal exosomal specific marker NCAM-L1 in NEs. **c**, Quantification of NCAM-L1 signal intensity normalized to total protein. Data points represent single PD (red) or control (black) individuals (*n*=6). **d**, Representative comparison between EVs-containing samples and samples containing NEs using western blot. An anti-NCAM-L1 antibody was used for the detection of NEs (~220, ~120 kDa). Synaptophysin as another neuronal marker is also shown (~30 kDa). CBB was used as loading control. **e**, **f**, Quantification of NCAM-L1 and synaptophysin after normalization to CBB (*n*=6). Data are shown as mean ± s.e.m. and statistical significance was determined by unpaired two-tailed Student's t-test and/or one-way ANOVA with Tukey multiple comparison test. n.s. not significant, *p<0.05, **p<0.01 and ****p<0.0001.

548 Figure 3

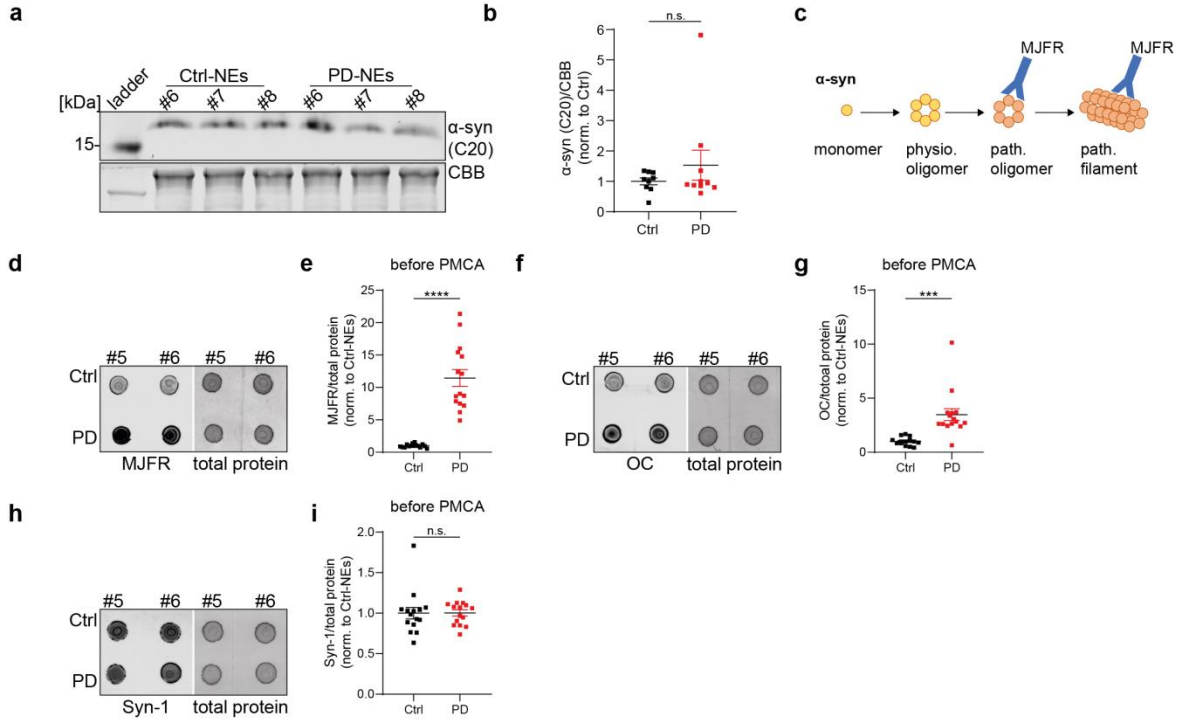

549

550 **Figure 3:** Detection of different α-synuclein (α-syn) forms within NEs.

551 **a**, Representative immunoblot of NEs-containing samples of PD and control individuals using
552 an anti-α-syn antibody. CBB was used as loading control. **b**, Quantitative analysis of C20
553 antibody (detects monomeric α-syn) signal intensity normalized to CBB. Each data point
554 represents one PD (red) or control (black) individual (*n*=8). **c**, Schematic demonstration of
555 the different structural conformations of α-syn. In its native form, α-syn presents as soluble
556 monomer or physiological (physio.) oligomer. Under pathological conditions the
557 oligomerization and fibrillization were triggered. The MJFR antibody detects pathological
558 (path.) oligomeric/filamentous α-syn conformations. **d**, Representative dot blot of PD-NEs
559 and Ctrl-NEs after staining with the MJFR antibody. Total protein was used as loading
560 control. **e**, Respective densitometry of MJFR antibody signal intensities of analyzed PD (red)
561 and control (black) subjects (*n*=15). **f**, Representative dot blot of PD-NEs and Ctrl-NEs using
562 the OC antibody that detects amyloid protein structures. **g**, Quantification of OC antibody
563 signal intensities. Each PD sample is shown as red data point, each control sample is shown
564 as black data point (*n*=15). **h**, Representative dot blot of PD-NEs and Ctrl-NEs using the Syn-
565 1 antibody (not confirmation specific). **i,** Respective densitometry of Syn-1 antibody signal
566 intensities of analyzed PD (red) and control (black) individuals (*n*=15). Further dot blots and
567 their analyses are shown in Extended Data Fig. 3j-o. Data are shown as mean ± s.e.m. and
568 statistical significance was determined by unpaired two-tailed Student's t-test. n.s. not
569 significant, ***p<0.001 and ****p<0.0001.

Figure 4

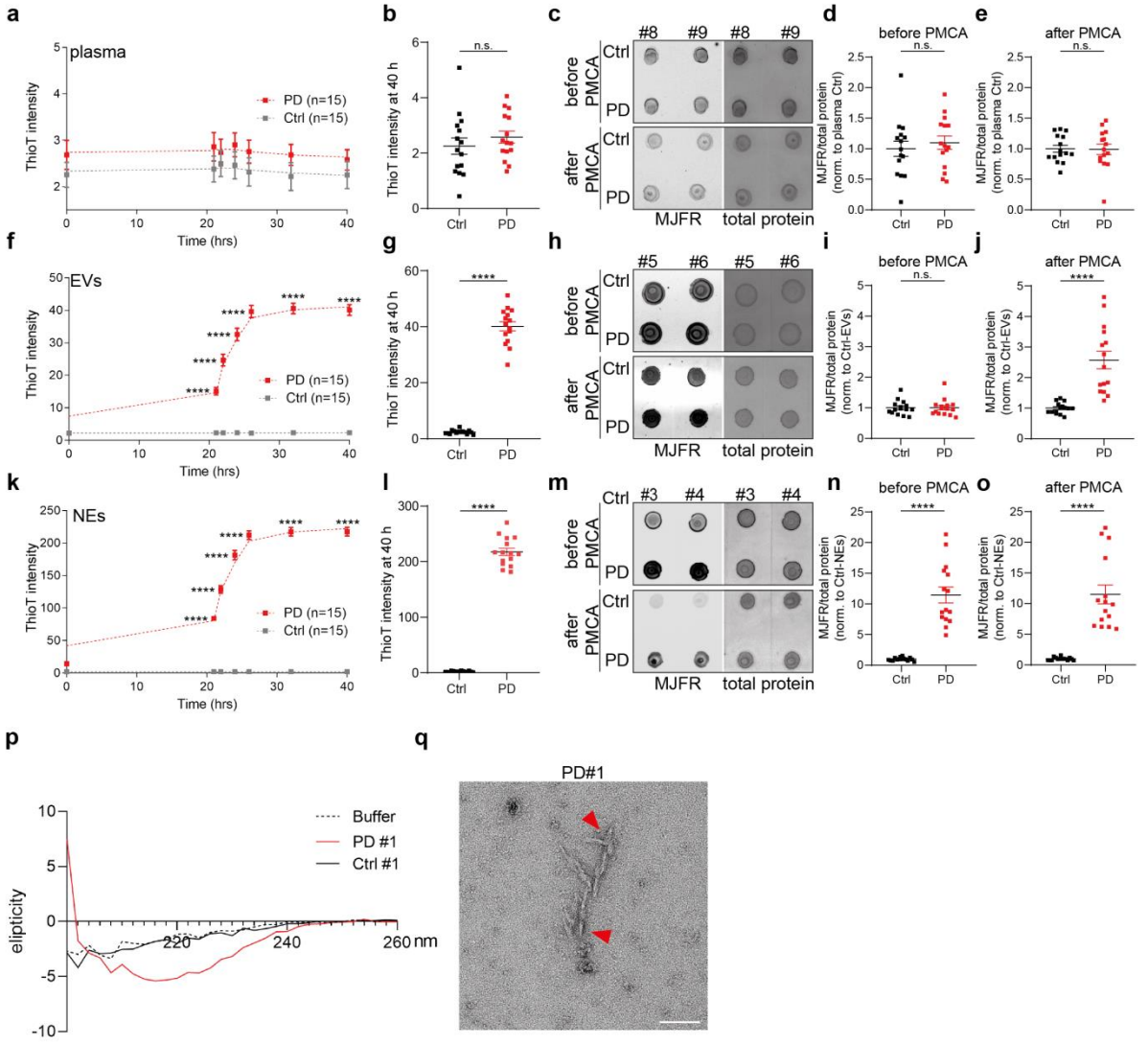

Figure 4: Amplification and characterization of pathological α-syn derived from NEs.

a, Total Thioflavin T (ThioT) signal intensity over time during the sixth round of protein misfolding cyclic amplification (PMCA) assay utilizing untreated plasma samples derived from PD patients (red) and control subjects (grey) (*n*=15). Data are shown as smoothed curves of total ThioT signals (mean ± s.e.m.) of combined individual measurements of 15 PD and 15 control samples for each time point. **b**, Analysis of total ThioT signal after 40 h PMCA as shown in Fig. 4a. Each data point represents a PD or control individual (*n*=15). **c**, Representative dot blot of untreated plasma samples of PD and control subjects (PD#8-#9, Ctrl#8-#9) before and after sixth round of PMCA using the MJFR antibody. Total protein was used as loading control. **d**, **e**, Respective densitometry of MJFR antibody signal intensities of all 15 analyzed PD (red) and 15 control (black) samples after normalization to total protein. **f**, Total ThioT signals over time during sixth round of PMCA of plasma-derived EVs from PD patients (red) and controls (grey) (*n*=15). **g**, Total ThioT signals of each tested subject after 40 h PMCA. **h**, Representative immunoblot of EVs of PD and control subjects (PD#5-#6, Ctrl#5-#6) before and after sixth round of PMCA using the MJFR antibody. Total protein was used as loading control. **i**, **j**, Quantification of MJFR antibody signal intensities of the

analyzed PD (red) and control (black) individuals after normalization to total protein (*n*=15). **k**, Total ThioT signal intensity of PD-NEs (red) and Ctrl-NEs (grey) is shown as smoothed curves over 40 h during the sixth round of PMCA. For each time point measurements of all 15 PD patients and all 15 controls were combined and demonstrated as means ± s.e.m. For PD samples a sigmoidal increase in ThioT signal is shown, whereas no increase in ThioT signal for control samples could be observed. **l**, Analysis of total ThioT signal after 40 h PMCA as shown in Fig. 4k. Each data point represents a PD or control individual (*n*=15). **m**, Representative dot blot of PD-NEs and Ctrl-NEs (PD#3-#4, Ctrl#3-#4) before and after sixth round of PMCA and staining with the MJFR antibody. **n**, **o**, Analyses of MJFR antibody signal intensities normalized to total protein. PD samples are shown as red data points, control samples as black data points. Individual total ThioT signal curves of all analyzed samples (untreated plasma, EVs, NEs) of PD patients (red, *n*=15) and controls (grey, *n*=15) of sixth PMCA round are shown in Extended Data Fig. 3g-i. **p**, Representative circular dichroism (CD) spectroscopy of formed α-syn aggregates derived from sixth round of PMCA assay. PD-derived α-syn species (red) exhibit β-sheet rich structures as indicated by a minimum extension at around 210-220 nm (PD#1). Control sample subjected to six rounds of PMCA (black) show spectra of the unfolded α-syn (Ctrl#1). All single spectra of analyzed samples (PD#1-13, Ctrl#1-#13) are shown in Extended Data Fig. 3p. **q**, Silver staining of PMCA-products of PD samples and control subjects after the sixth round of PMCA (PD#4-#7, Ctrl#4-#7). For all analyzed 4 PD samples protein bands were visualized on the high of α-syn (~16 kDa). No α-syn was observed in the pellets of Ctrl samples. Corresponding silver staining of samples containing EVs are shown in Extended Data Fig. 3q. **r**, Representative transmission electron microscopy (TEM) image of PD NE-derived α-syn conformers after six rounds of PMCA (PD#1). Red arrows indicate fibrillary protein conformations. Scale bar = 100 nm. Representative TEM image of Ctrl PMCA end product of the sixth round can be found in Extended Data Fig. 3r. For statistical analyses unpaired two-tailed Student's t-test and two-way ANOVA with Sidak's multiple comparison test were applied with n.s. not significant and ****$p<0.0001$. Extended Data Fig. 3g-i shows an overview of individual datasets of the sixth PMCA round ThioT signal curves.

Methods

Patient samples

Fifteen Parkinson´s disease (PD) patients were recruited from the in- and outpatient clinic of the department of Neurology at the University Hospital Kiel. Additionally, 15 non-PD individuals were recruited (relatives of patients from the department and patients without any evidence of neuroinflammatory and neurodegenerative disorders). Here, all non-PD individuals are referred as control group. Inclusion criteria for PD patients were diagnosis of PD according to the UK Brain Bank Criteria. Exclusion criteria for both groups comprised (i) inability to perform written performed consent (i.e. Montreal Cognitive Assessment < 18 points) and (ii) other diseases affecting the central nervous system. The study protocol was approved by the local Committee on Ethics and Human Research (D442/2) at the University of Kiel (Germany). Venous blood was collected from the median cubital vein in heparin tubes. A total of two full tubes (2 x 7.5 ml) were collected from each patient and each control.

Hoehn & Yahr / MDS-UPDRS-III / Disease duration

The Hoehn & Yahr score and Movement Disorder Society Unified Parkinson's Disease Rating Scale Part 3 (MDS-UPDRS-III) were used to classify the severity of PD based on clinical symptoms. Both were assessed by clinical examination in the Department of Neurology at the University Hospital Kiel at the time of blood collection. The disease duration was indicated in years and calculated from the year of initial diagnosis to the date of blood collection. An overview of Hoehn & Yahr score, MDS-UPDRS-III score and disease duration of each single PD patient can be found in Extended Data Table 1.

Isolation of extracellular vesicles (EVs)

After the blood samples were collected in heparin tubes, the blood was incubated for 10 min at room temperature. Next, samples were centrifugated at 2,500 x g for 10 min at 22 °C (Eppendorf Centrifuge, 5417R). Supernatants were transferred to low binding tubes (Sarstedt, #72.706.600) as 500 µL aliquots and were stored at -80 °C. Plasma samples were then centrifuged at 2,000 x g for 20 min at 22 °C to remove cells and debris. Supernatants containing the partially clarified plasma were transferred to new low binding tubes. Through the next centrifugation step (10,000 x g, 20 min, 22 °C) debris were removed. The required volume of clarified plasma was transferred to new tubes, phosphate-buffered saline (PBS) was added in equal parts and samples were mixed using a vortex mixer (MS2 minishaker, IKA, Germany). 150 µL of the Exosome Precipitation Reagent (Thermo fisher, #4484450) was added to each plasma sample. After 10 min of incubation at room temperature samples were centrifuged at 10,000 x g for 5 min at 22 °C. Supernatants were discarded and the exosome-containing pellets were resuspended. For immunoblotting and protein misfolding cyclic amplification (PMCA) assay pellets were resuspended in 30 µL in Triton buffer (1 % Triton-X100, 10 % glycerol, 150 mM NaCl, 25 mM HEPES at pH 7.4, 1 mM EDTA, 1.5 mM $MgCl_2$) containing 10 % protease inhibitor cocktail (cOmplete Protease Inhibitor Cocktail, Roche, #11836145001), 50 mM NaF, 2 mM $NaVO_4$ and 1 mM PMSF. For transmission electron microscopy (TEM) imaging and dynamic light scattering (DLS) measurements pellets were resuspended in 50 µL NaCl (0.9 %). For immunoblot analyses samples were incubated for 30 min on ice. After centrifugation for 5 min at 4 °C for 2,100 x g supernatants

were centrifuged through ultracentrifugation at 100,000 x g for 30 min at 4 °C (Beckman OptimaTM TLX Ultracentrifuge, Instrument-Typ CO-TLX 120). Supernatants were used for further analyses. Concentrations were measured by bicinchoninic acid assay (BCA) (Pierce).

Purification of neuron-derived exosomes (NEs)

Exosomes were resuspended in 300 µL PBS. Exosome resuspensions were incubated at 4 °C rotation overnight with 2 µg anti-NCAM-L1 antibody (Santa Cruz, #sc-514360). Beads (Protein A/G PLUS-Agarose, Santa Cruz, #sc-2003, lot nr. J0920) were blocked in 2 % bovine serum albumin (BSA) and incubated at 4 °C rotation overnight. The next day, blocked beads were washed using mild lysis buffer (40 mM HEPES, 7.4 pH), 120 mM NaCl, 1mM EDTA, 0.3 % CHAPS, 10 % glycerol). For each sample 30 µL mild lysis buffer was added to the beads. Washed and blocked beads were added to the exosome resuspensions with antibodies for 4 h at 4 °C with rotation. After collecting the immunoprecipitates by centrifugation at 1,000 x g for 5 min at 4 °C supernatants were discarded. Pellets were washed using mild lysis buffer. Following the last centrifugation step pellets were resuspended in Triton buffer (1 % Triton-X100, 10 % glycerol, 150 mM NaCl, 25 mM HEPES at pH 7.4, 1 mM EDTA, 1.5 mM $MgCl_2$) containing 10 % protease inhibitor cocktail (cOmplete Protease Inhibitor Cocktail, Roche, #11836145001), 50 mM NaF, 2 mM $NaVO_4$ and 1 mM PMSF. Samples were incubated for 30 min on ice before resuspensions were centrifuged through ultracentrifugation at 100,000 x g for 30 min at 4 °C (Beckman OptimaTM TLX Ultracentrifuge, Instrument-Typ CO-TLX 120). Supernatants were used for further analyses. For TEM imaging and DLS measurements pellets were resuspended in 50 µL NaCl (0.9 %). Concentrations were measured by BCA (Pierce).

Lysis of samples/Native dot blot analysis

After sequential protein extraction utilizing ultracentrifugation as described in Zunke et al. (100,000 x g, 30 min, 4 °C, Beckman OptimaTM TLX Ultracentrifuge, Instrument-Typ CO-TLX 120) soluble fractions were used for BCA protein assay [61]. Plasma samples, EVs and NEs were subjected to immunoblot analyses (dot blot, western blot). For dot blot analyses 7.5 µg of total protein were applied in 2.5 µL dots onto nitrocellulose membranes (#10600001, Amersham Biosciences), air-dried for 5 h and blocked in Tris-buffered saline (TBS) with 5 % (w/v) nonfat dry milk for 1 h. Primary antibodies (see Extended Data Table 2) were incubated overnight in TBS-Tween (1 %) containing 5 % nonfat dry milk. Secondary fluorescent-conjugated antibodies (see Extended Data Table 2) were incubated for 1 h after washing the membranes with TBS-Tween (1 %). Detection and digitalization were carried out using the Amersham Typhoon Biomolecular Imager (GE Lifesciences). Samples were dot-blotted under native conditions for structure specific readouts. As loading control total protein staining was used (Direct Blue 71, Sigma-Aldrich, #212407). Antibody signal intensities were normalized to loading control (total protein).

SDS PAGE/Western blot analysis and silver staining

For SDS-PAGE analyses samples (lysed as described above) were boiled with 5 x Laemmli buffer (250 mM TRIS/HCl, pH 6.8, 10 % SDS, 50 % glycerol, 0.5 % bromphenol blue and freshly added 5 % 2-mercaptoethanol). Total volume of each sample (~5 µl, 10/20 µg) was loaded on 10 % Tris-glycine gel and subjected to electrophoresis utilizing Thermo Fisher Scientific electrophoresis chambers (Mini gel tank, #A25977). Proteins were transferred to PVDF membranes (Merck Millipore, #IPFL00010). Membranes were fixed with 0.4 % paraformaldehyde in PBS for 20 min and blocked in TBS (1 %) with 5 % (w/v) nonfat dry milk for 1 h. Primary antibodies (see Extended Data Table 2) were incubated overnight at 4 °C and detection was performed after using secondary fluorescent-conjugated antibodies (see Extended Data Table 2) for 1 h at room temperature. Detection was carried out by the Amersham Typhoon Biomolecular Imager (GE Lifesciences). Coomassie staining of the gels (incubation in 0.02 % Coomassie Brilliant Blue G-250 Dye (Thermo Scientific™, #20272), 10 % ethanol (96 %), 2 % ortho-phosphoric acid (100 %), 5 % aluminiumsulfat-(14-18)-hydrat) was used as a loading control.

Silver stainings of SDS gels was performed as described in the manufacturer's protocol (Pierce, #24612).

Preparation of recombinant α-synuclein (α-syn)

Human recombinant monomeric α-syn was utilized and prepared as previously described [62]. In brief, by bacterial transformation of the human α-syn PT7-7 construct (gift from Dr. Hilal Lashuel, Addgene plasmid #36046; RRID: Addgene_36046 [63]) human α-syn was expressed in E. coli BL21 (DE3) pLysS competent cells (Novagen). Next, recombinant α-syn was isolated from E.coli by several purification steps, which include boiling and ion exchange chromatography (Resource-Q 6 ml column (GE Healthcare)). Subsequently, monomeric α-syn was purified by size exclusion chromatography using a SuperdexTM 75 10/300 column (GE Healthcare). The preparation of α-syn fibrils was carried out by agitation (1,000 rpm) of monomeric α-syn in a concentration of 3.4 µg/µl with a 3 mm polytetrafluoroethylene (PTFE) bead (Polyscience) in a Tris/HCl buffer (0.1 M, pH 7.4). Successful fibril formation was validated by measurement of Thioflavin T (ThioT) fluorescence.

Protein misfolding cyclic amplification (PMCA) assay

To amplify pathological α-syn forms from exosomes, 10 µg total protein of control and PD samples were incubated with 100 ng of recombinant monomeric α-syn in a total volume of 100 µl PBS in a dark 96-well plate (#237108, Thermo Fisher Scientific). After covering the plates with silicon lids (Thermo Fisher Scientific, #AB0566) and PARAFILM® M sealing film (Bemis, USA) they were incubated at 37 °C and constantly agitated at 1,000 rpm using a plate shaker (MTS 4, IKA). Before each measurement repeatedly 1 µl ThioT (1 mM stock solution, freshly prepared before each measurement) was added. ThioT fluorescence was monitored over time at indicated time points and measured at excitation of 410 nm and emission of 475 nm using a microplate reader (Gemini-EM, Molecular Devices). Measurements were stopped when ThioT fluorescence plateaued. For second/third/fourth/fifth and sixth rounds of PMCA amplification, 10 µl of the amplified end product of the round before were added to 100 ng of recombinant α-syn in a total volume of 100 µl PBS and subjected to agitation as described above. Pre-formed α-syn fibrils (10 µl of

0.68 ng/µl) and the presence of 100 ng α-syn monomers were used as positive control. As negative control 100 ng α-syn monomers as well as pre-formed fibrils only (10 µL of 0.68 ng/µl; without monomeric α-syn) were used.

Analyses show total ThioT signals. For this purpose, the raw numbers of plate reader were used and are shown in arbitrary units. In Fig. 4 data are shown as smoothed curves of total ThioT signals (mean ± s.e.m.) of combined individual measurements of all 15 PD patients and 15 control samples for each time point.

TEM of vesicles and PMCA end products

Negative-stain TEM was performed as previously described [64]. Isolated and buffer exchanged (100 mM Tris–HCl, pH 6.8) samples containing EVs or NEs were diluted to the final concentration of 0.5 µg/µl and 3 µl were added on a previously glow discharged (25 mA, 30 s) carbon-coated electron microscopy (EM) grid (Electron Microscopy Sciences, Hatfield, United States) followed by incubation on EM-grid for 30 sec. Subsequently the sample solution was removed using filter paper and the EM-grid was contrasted for two times with 1 % aqueous uranyl acetate solution (Merck Millipore, Billerica, MA, United States). The excess of the stain solution was removed with filter paper and the EM-grid was air-dried. After transfer of the grid into a JEOL 1400 Plus TEM (JEOL Germany, Munich, Germany) operating at 100 kV, images were taken at a magnification of 30.000 x to 50.000 x. Size measurements were performed by utilizing ImageJ software (FIJI, version 2.0.0).

Dynamic light scattering (DLS)

EVs and NEs were isolated as described above and each sample was adjusted to 1 µg/µl protein concentration. Measurements were performed as described before [65]. Briefly, samples were prepared in triplicates, filled into precisions cells (Quartz SUPRASIL®, Hellma GmbH & Co. KG, Müllheim, Germany) and each was measured 10 times with a 90°scattering angle at 20°C using the Spectroscatter 201 (RiNA GmbH, Berlin, Germany).

Circular dichroism (CD) spectroscopy

Samples derived from the sixth round of PMCA were subjected to circular dichroism measurements after the end of PMCA (plateau phase). Samples were measured at room temperature using a JASCO J-720 CD spectropolarimeter (JASCO) with 0.5 nm path-length cuvettes (utilizing ~80 µL of PMCA sample). Spectra were recorded from 190-250 nm wavelengths.

Schematic illustration

The illustrations in Fig. 1a and Fig. 2a were created using Smart Servier Medical Art (http://smart.servier.com/), which is licensed under CC BY 3.0.

785 Quantification and statistical analyses

786 Signal intensities of immunoblot analyses were quantified by utilizing ImageJ software (FIJI,
787 version 2.0.0) using background subtraction. Regions of interest were drawn around the dots
788 and integrated density was measured. Antibody signals were normalized to total protein level
789 as loading control. Analyses and data management was done using Prism 7 (GraphPad
790 Software, Version 7.0a) and Excel (Microsoft, Version 15.33). Statistical analyses were
791 performed and graphs created using Prism 7 (GraphPad Software, Version 7.0a). Data
792 points and column data are depicted as mean ± s.e.m. as described in corresponding figure
793 legends. Unpaired two-tailed Student's t-test was used for pairwise comparison, one-way
794 ANOVA with Tukey multiple comparison test and two-way ANOVA with Sidak's multiple
795 comparison tests were used for group comparisons. For statistical analyses a Gaussian
796 distribution was assumed. Data are shown as mean and statistical significance was obtained
797 when *p<0.05, **p<0.01, ***p<0.001 and ****p<0.0001. Individual p-values as well as
798 *n*-numbers are mentioned in corresponding figures.

799

800 **Data availability**

801 All dot blot raw data of this study are available on request. All raw values for analyzed dot
802 blots and endpoints of measurements of PMCA as well as further additional informations are
803 also available on request.

804

805 **Acknowledgments**

806 We sincerely thank Prof. Dr. Stefan Rose-John and Prof. Dr. Paul Saftig for providing support
807 and infrastructure. Moreover, we thank Melanie Boss for excellent technical assistance. We
808 also gratefully acknowledge the commitment of patients and control individuals
809 in participating and donating blood samples. This work was supported by the following
810 grants: ParkinsonFonds Germany to D.B., F.Z.; Deutsche Forschungsgemeinschaft (DFG,
811 German Research Foundation), grant number 125440785 – SFB 877, B11 to F.Z.

812

813 **Author contributions**

814 A.K., D.B. and F.Z. obtained funding and conceptualized the study; A.K., H.K. and E.S.
815 recruited and assessed patients and obtained plasma samples; P.A., S.B., J.B., A.D., A.K.,
816 W.L. and F.Z. performed experiments.; W.X. generated and provided α-syn monomer; D.B.,
817 A.K. and E.S. wrote the original manuscript; D.B., S.R.J., P.S., R.L. and F.Z. provided
818 support and infrastructure. All authors provided critical revision of the manuscript.

819

820 **Competing interests**

821 The authors declare no competing interests.

822

Additional information

Correspondence should be addresses to Annika Kluge, Department of Neurology, University Hospital Kiel, Kiel, Germany; Annika.Kluge@uksh.de or Friederike Zunke, Department of Molecular Neurology, University Hospital Erlangen, Friedrich-Alexander University Erlangen-Nürnberg, Erlangen, Germany; Friederike.Zunke@fau.de.

Extended Data Figures and Tables

Extended Data Table 1: Clinical parameters of each analyzed Parkinson´s disease (PD) patient (Movement Disorder Society Unified Parkinson's Disease Rating Scale Part 3, (MDS-UPDRS-III), Hoehn & Yahr score, disease duration) and controls were collected at the time of blood sampling. Shown are mean values, ranges and SD.

Sample number	Age/Sex	Diagnosis	Hoehn & Yahr	Disease duration (years)	UPDRS-III	Initial diagnosis (year)
PD 1	72/m	PD	2.5	13	32	2008
PD 2	78/m	PD	5	13	74	2008
PD 3	80/m	PD	2	7	8	2014
PD 4	61/m	PD	2	8	10	2013
PD 5	84/f	PD	2	2	21	2019
PD 6	46/f	PD	1	2	20	2019
PD 7	53/m	PD	1.5	2	15	2019
PD 8	82/m	PD	2.5	4	38	2017
PD 9	60/m	PD	2	11	31	2010
PD 10	55/m	PD	1	2	27	2019
PD 11	82/m	PD	2	3	22	2018
PD 12	65/f	PD	3	7	28	2014
PD 13	67/m	PD	3	3	48	2018
PD 14	73/f	PD	1	2	6	2019
PD 15	58/m	PD	1	1	20	2020
Mean	**67.7 (46-84)**		**2.1 (1.1)**	**3 (1-13)**	**26.7 (17.3)**	
Ctrl 1	85/m	healthy spouse	-	-	-	-
Ctrl 2	50/f	healthy spouse	-	-	-	-
Ctrl 3	79/m	post cardioembolic stroke	-	-	-	-
Ctrl 4	78/m	transient ischemic attack	-	-	-	-
Ctrl 5	54/m	transient ischemic attack	-	-	-	-
Ctrl 6	80/m	peripheral facial palsy	-	-	-	-
Ctrl 7	79/m	transient ischemic attack	-	-	-	-
Ctrl 8	70/m	post cardioembolic stroke	-	-	-	-
Ctrl 9	50/f	healthy spouse	-	-	-	-
Ctrl 10	72/m	relative of a patient	-	-	-	-
Ctrl 11	73/f	relative of a patient	-	-	-	-
Ctrl 12	79/f	transient ischemic attack	-	-	-	-
Ctrl 13	81/f	hypertensis crisis	-	-	-	-
Ctrl 14	69/f	transient ischemic attack	-	-	-	-
Ctrl 15	75/f	transient ischemic attack	-	-	-	-
Mean	**75 (50-85)**					

Extended Data Table 2: Overview of utilized antibodies

Antibody	Dilution	Application	Company (order no.)
Primary antibodies			
Anti-α-syn-filament [MJFR-14-6-4-2] (rabbit) Specificity: Conformational; Immunogen: α-syn filament; Epitope: aa133-138(Kumar et al., 2020)	1:1,000	Dot blot	Abcam (#209538), lot no. GR3256670-1
Anti-Amyloid Fibrils OC (rabbit) Specificity: Conformational; Immunogen: Fibrils from human Aβ42 peptide	1:1,000	Dot blot	EMD Millipore (#AB2286), lot no. 2876097
Anti-α-syn (Syn-1), Clone 42 (mouse) Specificity: Sequence; Immunogen: Rat α-syn; Epitope: aa91-99(Kumar et al., 2020)	1:1,000	Dot blot	BD Biosciences (#610787), lot no. 9192612
Anti-C20 (rabbit) Epitope: aa-120-140	1:1,000	Western blot	Santa Cruz (#sc-7011-R)
Anti-NeuN, Clone A60 (mouse)	1:1,000	Dot blot	EMD Millipore (#MAB377), lot no. 3156748
Anti-NSE-P1 (mouse)	1:1000	Western blot	BioLegend (#804901), lot no. B294828
Anti-CD63 (rabbit)	1:1000	Western blot Dot blot	Biozol (#EXOAB-CD63A-1), lot no. 200323-001
Anti-NCAM-L1 (C-2) (mouse)	1:50	Western blot Dot blot	Santa Cruz (#sc-514360), lot no. E1517
Anti-Synaptophysin, Clone SY38	1:1000	Western blot	Merck Millipore (#MAB5258), lot no. 2446868
Anti-hemoglobin beta (37-8) (mouse)	1:500	Dot blot	Santa Cruz (#sc-21757), lot nr. H0912
PGP9.5	1:500	Western blot	Origene (#UM870136), lot nr. F001
Secondary antibodies (fluorescent labelled)			
AlexaFluor 680 goat-anti-mouse	1:10,000	Western blot Dot blot	Thermo Fisher Scientific (#A21058), lot no. 1975023
AlexaFluor 680 donkey-anti-rabbit	1:10,000	Western blot Dot blot	Thermo Fisher Scientific (#A10043), lot no. 1917929
IRDye 800CW donkey-anti-rabbit	1:10,000	Western blot Dot blot	Li-Cor Biosciences (#926-32213), lot no. C80125-15
IRDye 800CW donkey-anti-mouse	1:10,000	Western blot Dot blot	Li-Cor Biosciences (#926-32212), lot no. C80829-05
Donkey-anti-goat IgG H&L (Cy3) reabsorbed	1:10,000	Western blot Dot blot	Abcam (#ab6949), lot no. GR314740-21
AlexaFluor 555 donkey-anti-rabbit	1:700	Immuno-histochemistry	Thermo Fisher Scientific (#A31572), lot no. 1454443
AlexaFluor 488 donkey-anti-mouse	1:700	Immuno-histochemistry	Thermo Fisher Scientific (#A21202), lot no. 1305303

838 Extended Data Figure 1

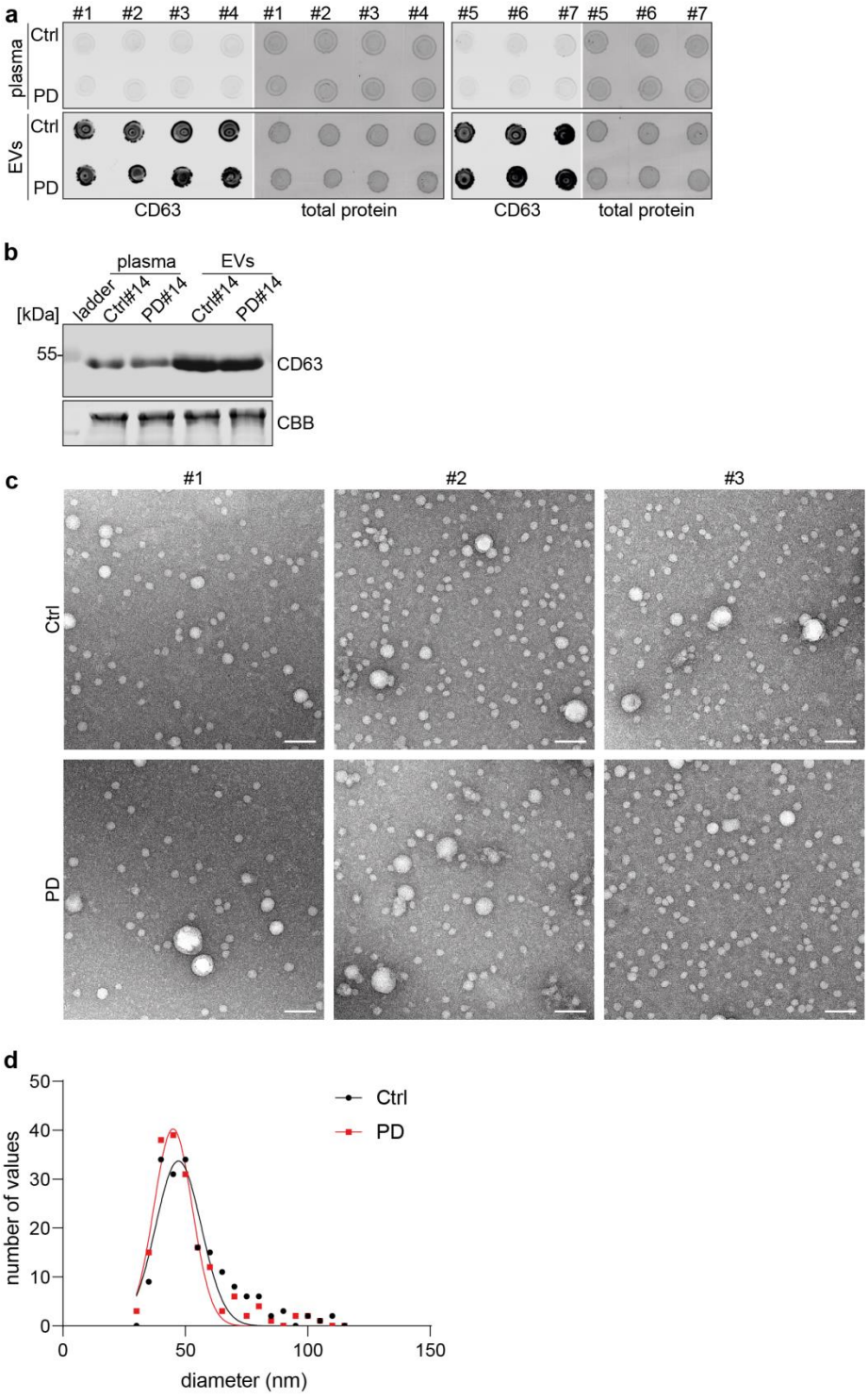

839

840 **Extended Data Figure 1:** Analyses of plasma-derived extracellular vesicles (EVs) from PD
841 patients and controls.

842 **a**, Representative immunoblot of untreated plasma samples and EVs after staining with
843 anti-CD63 antibody. Coomassie Brilliant Blue staining (CBB) was used as loading control
844 (*n*=2). **b**, Dot blot analyses of untreated plasma samples and EVs of 7 PD patients and
845 7 controls using an anti-CD63 antibody. Total protein was used as loading control. **c**,
846 Transmission electron microscopy (TEM) images of PD-EVs and Ctrl-EVs. Scale bar =

100 nm. **d**, TEM-based particle size analyses of EVs samples of 3 PD patients (red) and 3 controls (black). Shown are the quantities of EVs depending on their measured diameters (nm) as smoothed curves.

Extended Data Figure 2

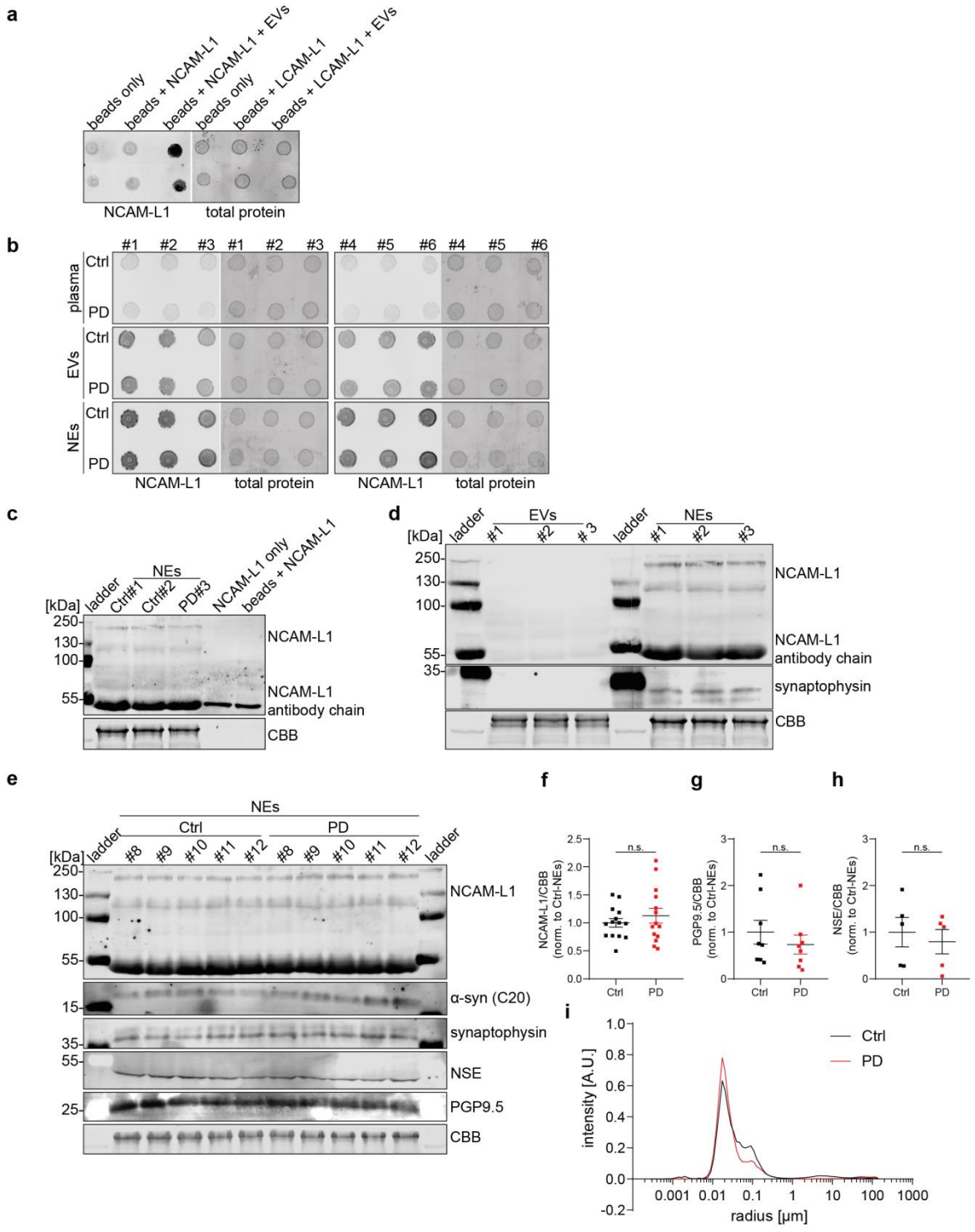

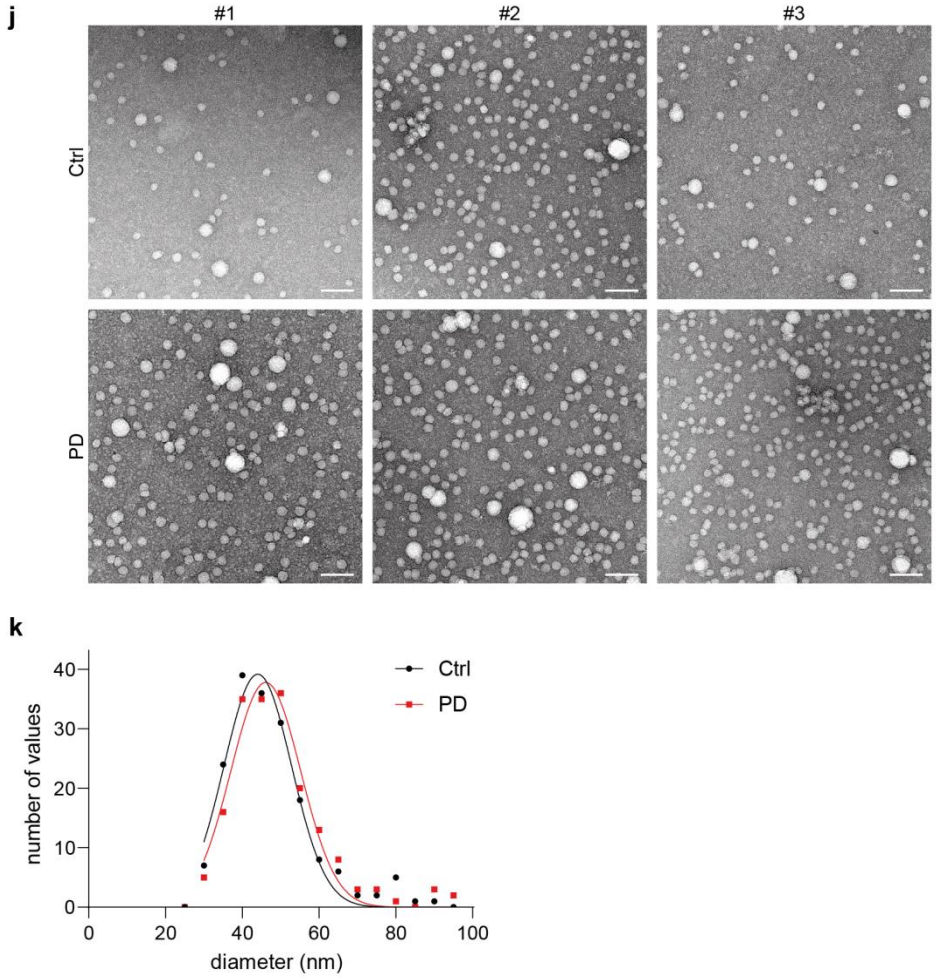

Extended Data Figure 2: Confirmation of the presence of neuron-derived exosomes (NEs).

a, Representative dot blot of end products after isolation of NEs using an anti-L1 cell adhesion molecule (NCAM-L1) antibody. As negative controls beads without precipitating antibody (beads only) and beads with precipitating antibody (beads + NCAM-L1) were examined. As positive control isolated human EVs were used and beads as well as precipitating antibody were added (beads + NCAM-L1 + EVs). Total protein was used as loading control. **b**, Representative dot blot of untreated plasma samples, EVs and NEs of 6 PD patients and 6 controls after staining with an anti-NCAM-L1 antibody. Total protein was served as loading control. **c**, Representative immunoblot of end products after using the protocol of isolating NEs. Shown are positive controls (beads + NCAM-L1 + human EVs) and negative controls (NCAM-L1 only; beads + NCAM-L1). **d**, Total immunoblot from Fig. 2d. Shown are representative EVs and NEs samples after staining with an anti-NCAM-L1 antibody. **e**, Representative western blot of NEs of PD patients and controls using diverse antibodies to detect different neuronal markers and α-synuclein (NCAM-L1, synaptophysin, neuron-specific enolase (NSE), protein gene product 9.5 (PGP9.5), C20 (detects monomeric α-syn)). CBB was used as loading control. **f-h**, Quantification of shown signal intensities of NCAM-L1 (n=14), PGP9.5 (n=8) and NSE (n=5) after normalization to CBB. Each data point represents a single PD patient (red) or control subject (black). **i**, Representative dynamic light scattering (DLS) measurements of isolated NEs of 3 PD patients (red) and 3 controls (black), shown as smoothed curves. **j**, Representative TEM images of PD-NEs and Ctrl-NEs. Scale bar = 100 nm. **k**, TEM-based particle size analyses of EVs samples of 3 PD patients (red)

874 and 3 controls (black). Shown are the quantities of NEs depending on their measured
875 diameters (nm).

Extended Data Figure 3

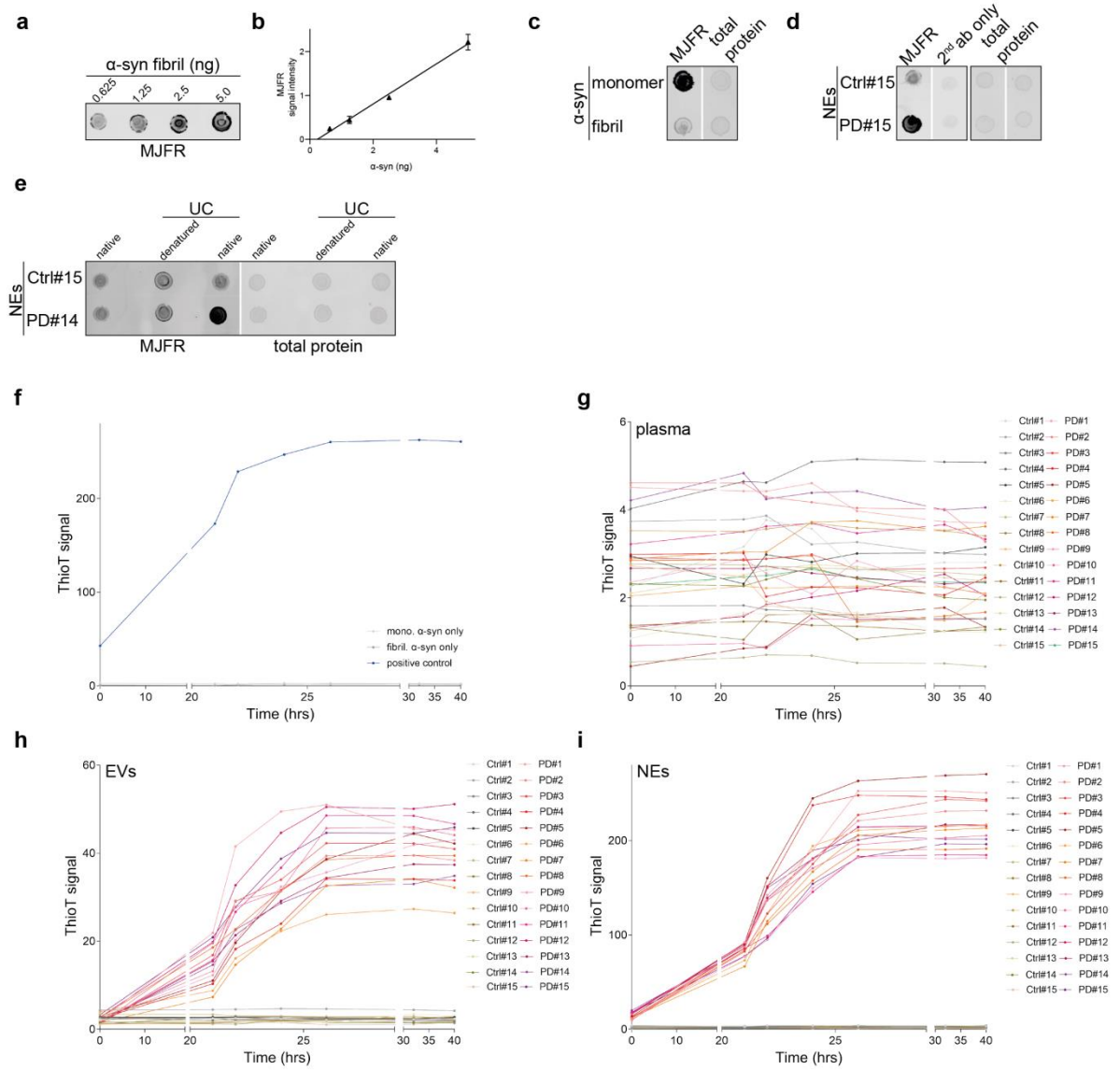

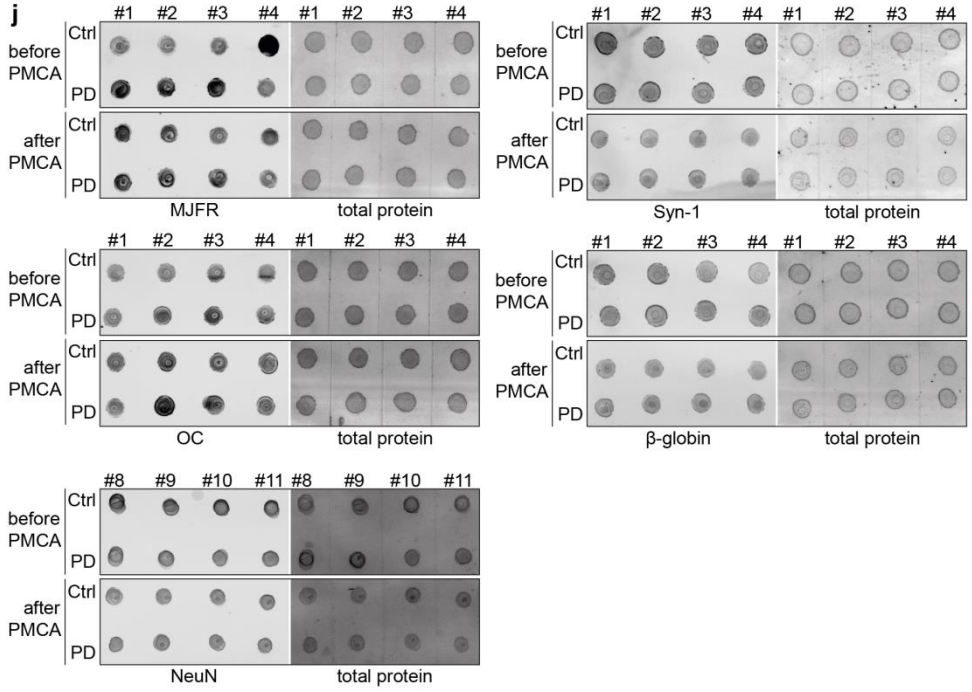
j
#1 #2 #3 #4 #1 #2 #3 #4
before PMCA
after PMCA
Ctrl
PD
MJFR
total protein
Syn-1
β-globin
OC
#8 #9 #10 #11 #8 #9 #10 #11
NeuN

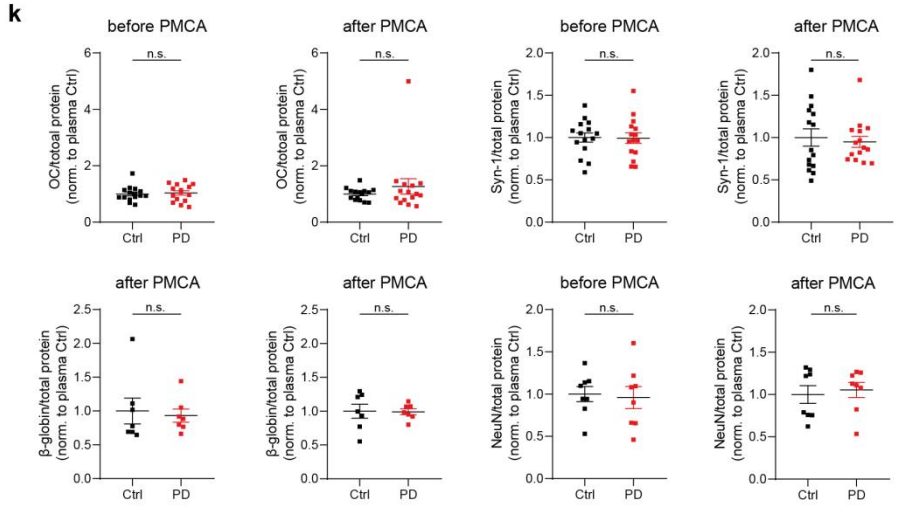
k
before PMCA
after PMCA
n.s.
OC/totoal protein (norm. to plasma Ctrl)
Syn-1/total protein (norm. to plasma Ctrl)
β-globin/total protein (norm. to plasma Ctrl)
NeuN/total protein (norm. to plasma Ctrl)
Ctrl
PD

878

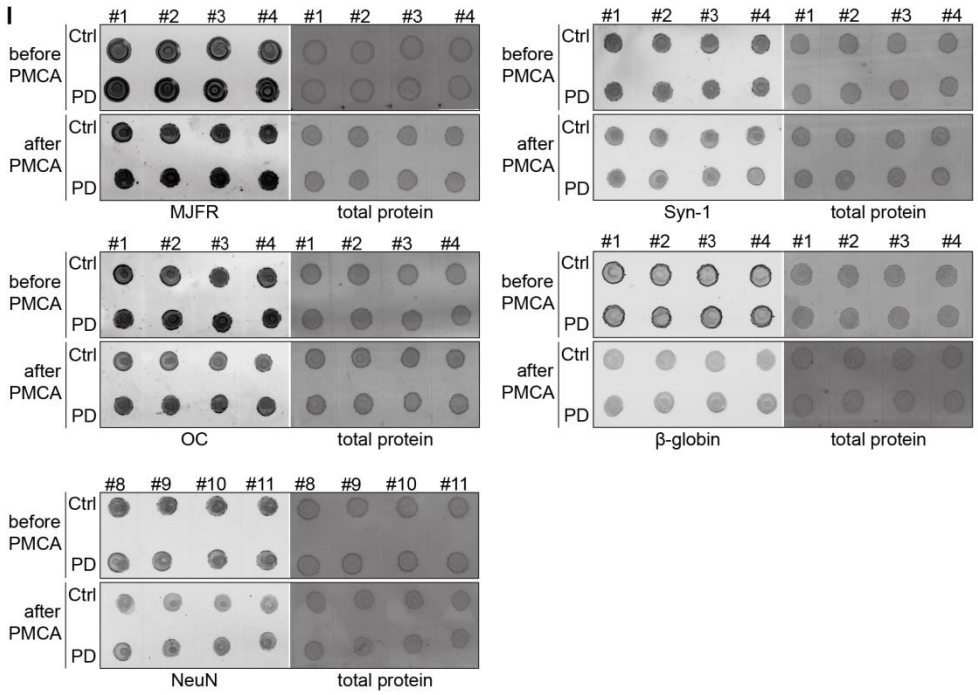
l
#1 #2 #3 #4 #1 #2 #3 #4
before PMCA
after PMCA
Ctrl
PD
MJFR
total protein
Syn-1
OC
β-globin
#8 #9 #10 #11 #8 #9 #10 #11
NeuN

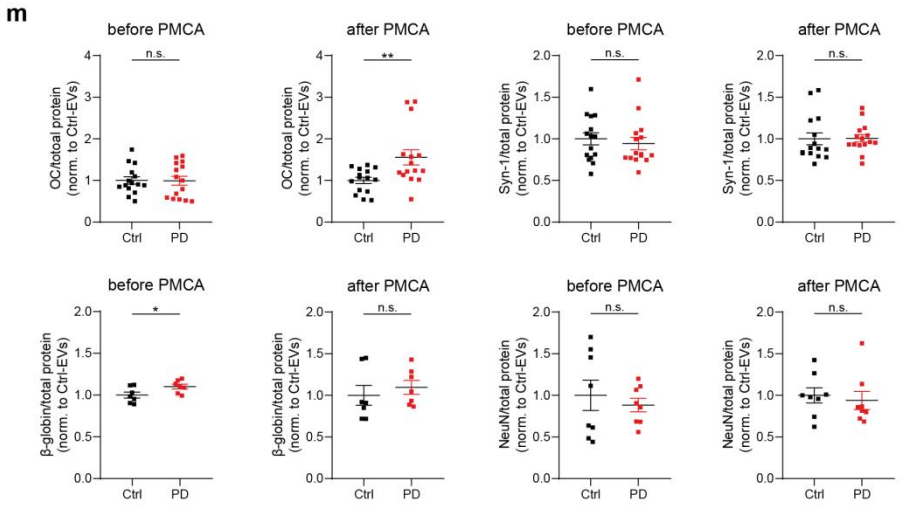
m
before PMCA
after PMCA
OC/totoal protein (norm. to Ctrl-EVs)
Syn-1/total protein (norm. to Ctrl-EVs)
β-globin/total protein (norm. to Ctrl-EVs)
NeuN/total protein (norm. to Ctrl-EVs)
n.s.
**
*
Ctrl
PD

879

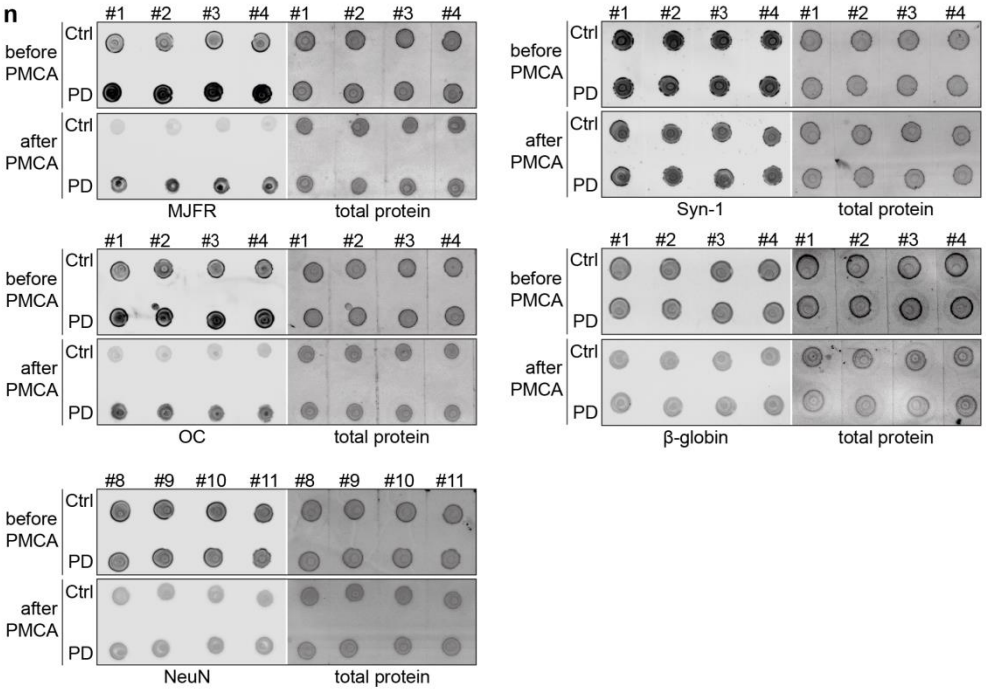

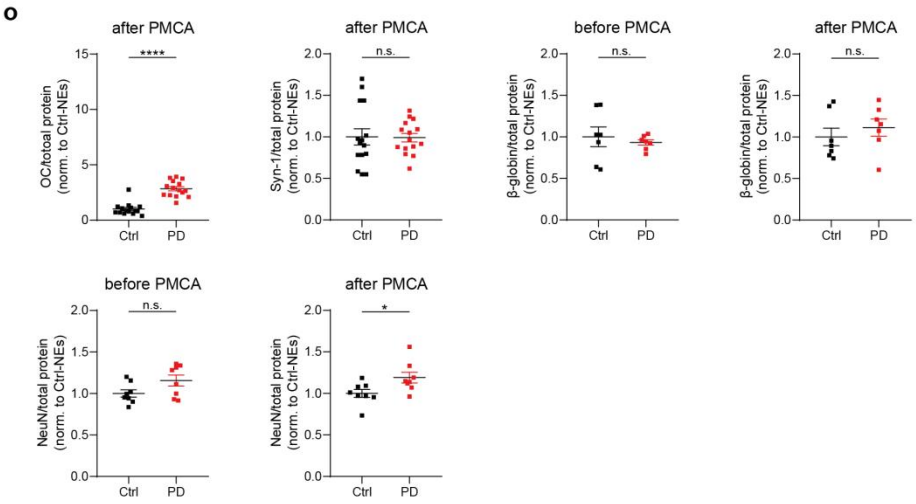

880

881

882

883

884

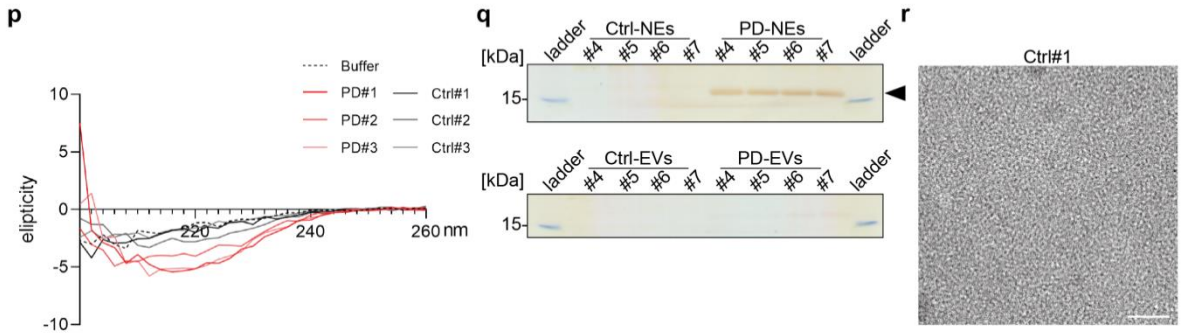

885

886 **Extended Data Figure 3:** Detection and amplification of neuronal α-synuclein (α-syn).

887 **a**, Analysis of MJFR antibody (detects pathological, oligomeric/filamentous α-syn
888 conformations) signal intensity of increasing concentrations of recombinant α-syn fibrils
889 (0.625-5.0 ng). **b**, Standard curve of MJFR signal intensity. The antibody binding is linear to
890 the concentration of α-syn fibrils ($y = 0.4568 * x + 0.1064$; $R^2 = 0.99$). **c**, Representative dot
891 blot of recombinant monomeric α-syn and recombinant fibrillary α-syn. Total protein was
892 used as loading control. **d**, Dot blot of PD-NEs and Ctrl-NEs to exclude unspecific binding
893 and false-positive signals of secondary antibody (anti-rabbit). MJFR as primary antibody
894 together with secondary antibody was utilized as control to proof signal differences between
895 PD#15 and Ctrl#15. Total protein was used as loading control. **e**, Representative dot blot
896 analysis of Ctrl#15 and PD#14 after different treatments (under native conditions and without
897 ultracentrifugation (UC); denatured and after ultracentrifugation; under native conditions and
898 after ultracentrifugation). Total protein was used as loading control. **f**, Total Thioflavin T
899 (ThioT) fluorescence of recombinant, pre-formed α-syn fibrils (input: 10 µl 0.68 ng/µl, 100 ng
900 monomeric α-syn) (blue) was used as positive control, α-syn monomers (without seed) (light
901 grey) and α-syn fibrils (without α-syn monomers) (dark grey) were used as negative controls.
902 **g-i**, Individual total ThioT signal curves over time of untreated plasma samples (g), EVs (h)
903 and NEs (i) of all analyzed PD patients (red, *n*=15) and controls (grey, *n*=15) subjected to
904 protein misfolding cyclic amplification (PMCA) assay. Each curve represents an individual
905 biological sample. **j**, **k**, Dot blot overview of further analyzed untreated plasma samples of PD
906 patients and controls. As antibodies the MJFR, OC (interacts with amyloidogenic protein
907 structure), Syn-1 (not confirmation specific), neuronal nuclear protein (NeuN) and ß-globin
908 antibodies were used. All samples were analyzed before PMCA and after the sixth round of
909 PMCA. Total protein was used as loading control. **k**, For analysis, antibody signal intensities
910 were quantified and normalized to loading control total protein. Each data point represents
911 one individual PD patient (red) or control (black). **l-m**, Also performed dot bots of EVs of PD
912 patients and controls before PMCA and after sixth round of PMCA. As described above,
913 MJFR antibody, OC antibody, Syn-1 antibody, anti-NeuN antibody and anti-ß-globin antibody
914 were used. Total protein staining was utilized as loading control. **m**, Analyses of shown
915 antibody signal intensities after normalization to total protein. PD samples are shown as red
916 data points, controls as black data points. **n**, Representative dot blots of PD-NEs and
917 controls before PMCA and after sixth round of seeding assay. **o**, Quantification of shown dot
918 blot analyses. Each data point represents a single PD patient (red) or control (black). **p**,
919 Circular dichroism (CD) spectra of α-syn aggregates derived from sixth round of PMCA
920 assay. NEs-derived α-syn species of PD samples (red/orange) exhibit β-sheet rich structures
921 as indicated by a minimum extension at around 220 nm. Control samples subjected to six
922 rounds of PMCA are shown in grey colours. **q**, Silver staining of PMCA products of PD-NEs

and Ctrl-NEs after the sixth round of PMCA. For all analyzed 4 PD samples protein bands were visualized on the high of α-syn (~16 kDa). No α-syn was observed in the pellets of the control samples. Corresponding silver staining of PMCA end products (sixth round) of PD-EVs and Ctrl-EVs is shown in the lower part of Extended Data Fig. 4q. **r**, TEM image of PMCA end product (sixth round) of Ctrl-NEs. Scale bar = 100 nm. For statistical analyses unpaired two-tailed Student's t-test and two-way ANOVA with Sidak's multiple comparison test were applied with n.s. not significant, *p<0.05, **p<0.01 and ****p<0.0001.